

# The Lower Bound for Glass Strength and Its Interpretation with Generalized Weibull Statistics for Structural Applications

Roberto Ballarini, F.ASCE<sup>1</sup>; Gabriele Pisano<sup>2</sup>; and Gianni Royer-Carfagni<sup>3</sup>

**Abstract:** Because the strength of glass is governed by randomly distributed surface flaws that can propagate catastrophically when the applied stress reaches a critical value, the weakest-link-in-the-chain rationale is the universally accepted interpretation of its significant variability. The two-parameter Weibull extreme value distribution is currently the most commonly used model for structural design, although it is recognized that it fails to capture the experimental data within the region of small failure probabilities, associated with the lowest strengths. However, the precise characterization of this left-hand-side tail of the distribution is crucial for structural applications, for which only very low probabilities of failure are accepted. Experiments have provided evidence of the existence of a lower bound for the strength of glass, a finding that, if proved, could revolutionize the approach to the safety of glass structures. Referring to the large-scale experimental program of the Technical Committee 129—Working Group 8 of the European Committee for Standardization (CEN/TC129/WG8), various generalized statistical distributions like Weibull, either prescribing a strength limit or not, are compared in their ability to interpolate the experimental data using the chi-square goodness-of-fit test. Arguments are presented that support the existence of a minimal strength, which can be reduced, but not annihilated, by the inevitable degradation of the glass surface produced by aging and in-service-related damage. DOI: 10.1061/(ASCE)EM.1943-7889.0001151. © 2016 American Society of Civil Engineers.

**Author keywords:** Structural glass; Strength; Fracture; Brittle failure; Weibull statistics; Abraded glass; Minimal strength.

## Introduction

Transparency has become a highly sought factor in architectural applications and has led to an increasing demand for flat glass in buildings. This demand for architectural glass, which accounts for approximately 80% of glass production, has increased by 5% per annum since 2009. Concomitantly, the role of architectural glass has expanded from that of window panes to load-bearing structural components. This shift makes it necessary to characterize the mechanical properties of glass as precisely as has been done for all other materials traditionally used in structural applications.

Glass is linear elastic, homogeneous, isotropic, and brittle. The nominal strength of glass is governed by the shape, size, and spatial distribution of surface flaws that are created during the manufacturing process, subsequent handling, and in-service conditions. Fracture results from the unstable propagation of a dominant crack when the combination of its size and the stress normal to its surfaces reaches a critical value. Moreover, cracks can grow

subcritically over time at stress levels much lower than the critical limit (Wiederhorn and Bolz 1970), a phenomenon generally referred to as *static fatigue* or *slow crack propagation*. Thus, the macroscopic strength depends upon time and is, indirectly, influenced by the thermo-hygrometric conditions (Wiederhorn et al. 1982), which affect the slow crack propagation speed.

It is important to understand how cracks are created on the surfaces of the flat glass components considered in this paper. Flat glass is typically made using the process patented by Sir Alastair Pilkington in the 1950s, which consists of pouring a glass paste on a bed of molten tin forming a floating panel, hence the name *float* glass. The surfaces become smooth on both sides, while the temperature is gradually reduced from 1100°C down to 600°C. Then, the panel is pulled off the bath by rollers and the glass sheet passes through a *lehr* where it is cooled gradually. Thus, internal stresses, which may be due to the rapid temperature change, are released at least partially. Surface defects are inevitably present especially on the tin-side surface, due to the contact with the tin bath and, even more so, with the rollers. Additional defects at the borders are also introduced by the cutting process. The size of the flaws is limited by strict factory production controls, mainly because an excessive amount of defects can reduce the transparency and, hence, the aesthetic quality price. Additional surface defects can develop over time. Despite being more resistant to corrosion than most structural materials, glass does age and weather. The microscopic peaks and dents that are present on its surfaces can enhance chemical reactions with contaminants. In addition, the hydrophilic properties of glass cause corrosion and increase surface roughness. Abrasion, another phenomenon that causes a reduction of glass performance, can result from the manufacturing and the transport processes, the impact of small hard objects carried by the wind, and, in desert areas, sandstorms.

Clearly, the random nature of the shape, size, and distribution of surface flaws bestows on glass a nondeterministic and structural size-dependent strength. The larger the loaded surface, the higher

<sup>1</sup>Professor and Chair, Dept. of Civil and Environmental Engineering, Cullen College of Engineering, Univ. of Houston, Cullen College of Engineering Bldg. 1, 4726 Calhoun Rd., Room N107, Houston, TX 77204-4003 (corresponding author). E-mail: rballarini@uh.edu

<sup>2</sup>Graduate Student, Dept. of Industrial Engineering, Univ. of Parma, Parco Area delle Scienze 181/A, I-43124 Parma, Italy. E-mail: gabriele.pisano@studenti.unipr.it

<sup>3</sup>Professor, Dept. of Industrial Engineering, Univ. of Parma, Parco Area delle Scienze 181/A, I-43124 Parma, Italy; Construction Technologies Institute, Italian National Research Council, Lombardia 49, I-20098 San Giuliano Milanese (Mi), Italy. E-mail: gianni.royer@unipr.it

Note. This manuscript was submitted on December 18, 2015; approved on June 16, 2016; published online on September 9, 2016. Discussion period open until February 9, 2017; separate discussions must be submitted for individual papers. This paper is part of the *Journal of Engineering Mechanics*, © ASCE, ISSN 0733-9399.

the probability of finding a microdefect of critical size (Vandebroek et al. 2014). On the other hand, if the state of stress is uniform and equibiaxial, there is 100% probability of one dominant crack being oriented so its surfaces are perpendicular to the direction of maximum tensile stress. For other states of stress, the Mode I opening stress may be less than the principal stress (Collini and Royer-Carfagni 2014). The various experimental campaigns confirm the dependence of strength upon size and type of stress, providing a further validation of the Weibull model. The statistical model chosen to interpret strength distributions should account for all these aspects. The Weibull distribution, which is based on the weakest-link-in-the-chain concept (Weibull 1939), is such a model and it has been generally favored for interpreting the variability in the measured strengths of glass and other brittle materials. The connection between the flaw distribution and the Weibull strength distribution was shown by Freudenthal (1968). The traditional approaches assume that cracks are randomly orientated, noninteracting, and shear insensitive. However, there are many variants of the model according to the chosen fracture criterion (Batdorf and Heinisch Jr. 1978).

The two-parameter Weibull distribution, which assumes a non-zero failure probability for all levels of tensile stress, is the most widely used for the structural design of components made of glass and other brittle materials. This model can provide accurate estimates of the expected mean and standard deviation of glass strength and may be sufficient for some ceramic components. However, there is a wealth of evidence that points to its inability to capture the experimental data associated with small failure probabilities (and lowest strengths) (Danzer 2006; Yankelevsky 2014; Pisano and Royer-Carfagni 2015a). It is precisely this left-hand-side tail of the distribution that must be characterized accurately in high reliability structural applications. For example, the Eurocode EN1990 assigns target failure probability values of the order of  $10^{-6}/10^{-7}$  in 1 year (CEN 2005). In this context, only the left-hand-side tail of the cumulative probability function of glass strengths is of importance. However, attempts at calibrating the material safety factors using the two-parameter Weibull distribution lead in general to very high values (Badalassi et al. 2014), much higher than those traditionally employed on the basis of practical and professional experience. This is also due to the very conservative rescaling of this statistical distribution that is employed to account for effects of size and stress state. As demonstrated by Le et al. (2015), while it is possible to define a two-parameter Weibull distribution that is on the safe side when calibrated using experimental data derived from specimens of a certain size and loading (Overend and Louter 2015), the model may not be conservative in its predictions of the strength distributions of specimens of different size and loading.

Improved models of the strength distribution of glass could increase the competitiveness of glass components in the construction industry by avoiding redundant design. This is why research on micromechanics-based statistical models, as alternatives to the two-parameter Weibull, is of great interest to the glass industry. Numerous statistical distributions have been developed in recent years. By assuming the existence of two distinct types of flaw populations on the same surface of a brittle material (Phani and De 1987), Klein (2011) proposed the use of a bimodal Weibull statistics, whose micromechanically motivated modeling is considered by Rickerby (1980). Another approach consists in adopting a three-parameter Weibull distribution (Przybilla et al. 2011a), which prescribes a lower bound for glass strength. However, questions have been raised about the existence of a threshold (Basu et al. 2009). Methods for the material calibration according to the three-parameter Weibull model are available in the literature (Przybilla et al. 2011b), possibly taking into account also the effects of sub-critical crack growth (Salviato et al. 2014). Moreover, experimental

results on predamaged glass (Madjoubi et al. 1999; Durchholz et al. 1995) have confirmed that the minimal strength of float glass can be reduced, but not annihilated, by the damaging process. Another noteworthy aspect is that the dispersion of the strength data of damaged glass is much narrower than in the pristine material.

By analyzing the results of the experimental campaign by CEN-TC129/WG8 recorded in 2006 (CEN 2006), which to the authors' knowledge represents the widest work for the characterization of the strength of float glass, this study attempts to interpolate the data with either bounded (left truncated or three-parameter) and unbounded (bilinear, bimodal, and extended) generalized Weibull distributions. The chi-square goodness-of-fit test is used to assess whether the discrepancy between experimental data and model prediction is due to chance alone. In addition, the effects of abrasion due to aging are discussed on the basis of micromechanically motivated considerations. This paper thus presents arguments that, albeit tentatively at this time, seem to support the existence of a lower bound for glass strength, which in the authors' opinion should be attributed to the limitation of defects, guaranteed by the factory production controls.

## Experimental Evidence of the Lower Bound for Glass Strength

Experimental results have provided a wealth of evidence that the distribution of bending strength of float glass systematically deviates from the prediction of the two-parameter Weibull model. In particular, the measured strengths at low failure probabilities are in general much higher. Experiments on artificially damaged specimens have confirmed a substantial drop in material strength with respect to the pristine material. However, as the damaging action is increased (either in strength or duration), the measured strength tends asymptotically to a nonzero limit value, while the dispersion of the data (standard deviation) decreases. A brief account of the most significant experimental campaigns is reviewed next, with particular attention given to the evidence that appears to confirm the existence of a lower limit of glass strengths.

### Experimental Campaign by CEN-TC129/WG8

The working group CEN/TC129/WG8 of the European Committee for Standardization (CEN) performed a wide experimental campaign consisting of 741 failure stress measurements (CEN 2006). Thirty samples produced by different European glass manufacturing plants, each one composed of approximately 25 plate specimens 6 mm thick, were tested according to the EN1288-2 standard (CEN 2001b). This experimental program formed the basis for the evaluation of the characteristic value of glass strength indicated in European standards and guidelines.

The method of EN1288-2 is a coaxial double ring (CDR) test configuration with additional overpressure in the area bounded by the inner ring (CEN 2001a), whose aim is to generate an almost uniform equibiaxial stress state in a circular region far from the borders. In these conditions, the surfaces of the dominant surface crack (Appendix) would always be perpendicular to the principal component of tensile stress, regardless of crack orientation. In addition, the most stressed region is far from the borders, where the severity of surface defects is enhanced by the cutting process (Rodichev et al. 2012). The overpressure is introduced to compensate for geometric nonlinearities, which are responsible of the deviation from equibiaxiality with respect to the linear elastic solution for the CDR configuration (Pisano and Royer-Carfagni 2015b). With the same purpose, standard ASTM C1499 (ASTM 2009) prescribes a CDR test with a geometry variable according

to the specimen thickness, in order to limit deflections and hence the geometric nonlinear effects.

Some critical points concerning this experimental method have been discussed previously (Pisano and Royer-Carfagni 2015b, a). Pisano and Royer-Carfagni (2015b) showed that the relationship proposed in EN1288-2 (CEN 2001a) between the induced radial tensile stress, the nominal glass pressure, and the piston force is not correct. Therefore, the values recorded (CEN 2006) are not representative of the maximum tensile stress on the specimen at failure. Moreover, the additional overpressure is not able to compensate for the deviation from equibiaxiality due to the nonlinear effects, hence the need of rescaling the experimental data. Following the procedure shown in Pisano and Royer-Carfagni (2015a), it is customary to rescale the values of the strength measured in the tests for the configuration of uniform equibiaxial state of stress on a unit ( $1 \text{ m}^2$ ) area, taken as the reference condition. Moreover, since during the float production process one side of the glass is exposed to air (air side), while the other side is in contact with the molten tin bath (tin side) and with the rollers, different kinds of surface defects are present on the two surfaces. This requires the use of two different statistics for the tin and the air sides (Pisano and Royer-Carfagni 2015a).

Fig. 1 shows, with a distinction between the tin and air sides, the cumulative probability distribution  $P_f$  of the strengths recorded (CEN 2006), corrected by considering the actual stress induced by piston force and overpressure calculated with a nonlinear finite-element method (FEM) model (Pisano and Royer-Carfagni 2015a). Data have been arranged in ascending order, assigning to each datum the experimental value of the probability of failure defined as  $P_f = i/(n + 1)$ , where  $i$  is the  $i$ th datum and  $n$  is the total number of data.

By plotting  $\ln[-\ln(1 - P_f)]$  versus  $\ln(\sigma)$  in the two-parameter Weibull plane (represented in the same figure), it is evident that the

left tails of the distributions cannot be interpolated by a straight line as required by the two-parameter Weibull distribution. This is a very stringent implication, since probabilities of failures that are admitted in construction works are very low, of the order of  $10^{-5} - 10^{-7}$  per year, so that the accurate interpretations on the left-hand-side tails is of major importance.

### Experiments on Artificially Damaged Glass

There are various contributions in the technical literature that record experimental campaigns where specimens have been conditioned in order to artificially reproduce the damaging effects of aging. Durchholz et al. (1995) performed tests according to EN1288-2 (CEN 2001a) and EN1288-5 (CEN 2001c) on float glass plates that had been pretreated by dropping corundum ( $\text{Al}_2\text{O}_3$ ) on them. The statistical analysis of the experimental data through a two-parameter Weibull model showed that predamage leads to a lower scale parameter and to a much greater scale exponent in the Weibull distributions. In other words, the strongest elements of the distribution are shifted to lower strength values, whereas the dispersion of the data is highly reduced. More specifically, the results showed that the minimum strength values remained of the same order as those obtained by analyzing the pristine float glass; however, such minimal values remained much higher than those predicted by a two-parameter interpolating Weibull statistics for undamaged specimens that was extrapolated to the very low fracture probabilities associated with structural standards.

To the authors' knowledge, a standardized method for predamage glass has not been defined. Indeed, the applicability of the process of Durchholz et al. (1995) is not definitive because it requires an impractical number of tests to estimate very low probability of failure. However, the experiments are very interesting, at least at the qualitative level, because they have convincingly

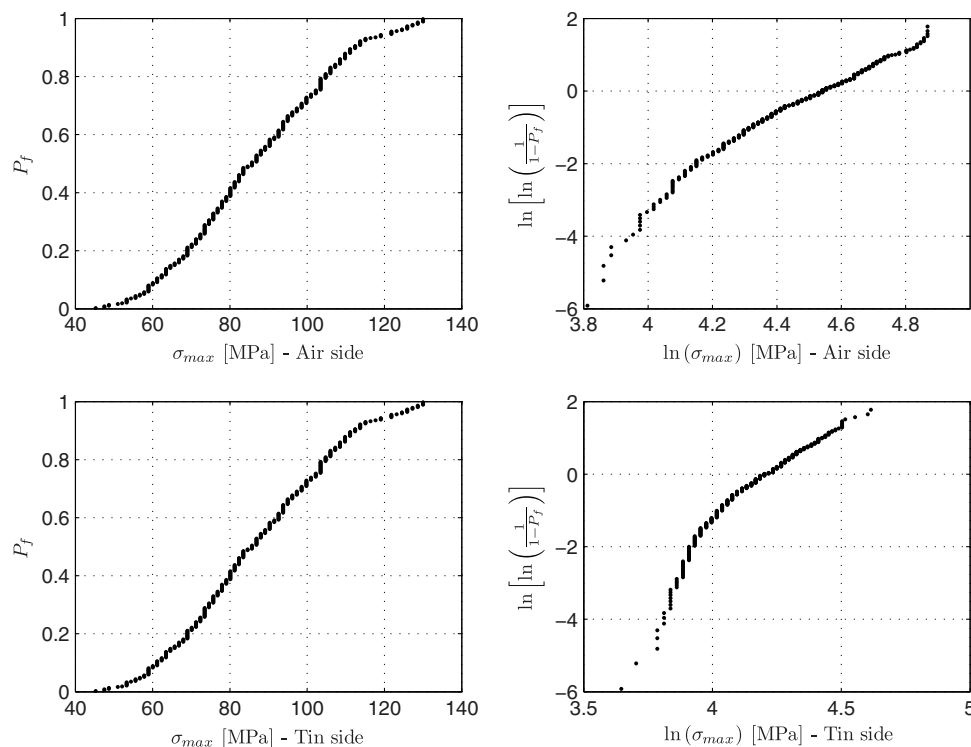


**Fig. 1.** Cumulative probability distributions of the strengths for the tin and air side, obtained by CEN-TC129 (CEN 2006), corrected to compensate the inaccuracy of EN1288-2 (CEN 2001b); same values plotted in the two-parameter Weibull plane

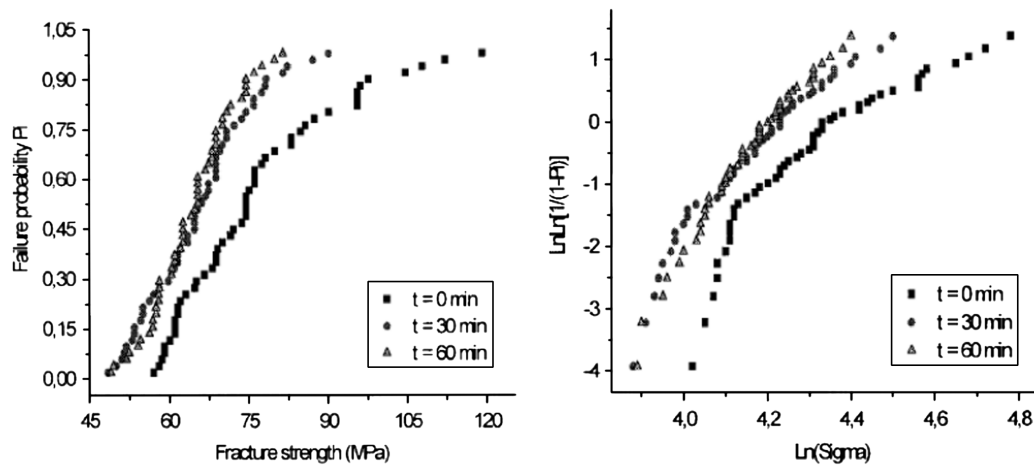


**Fig. 2.** Probability plots, in the Cartesian and Weibull planes, of the experimental data (Madjoubi et al. 1999); three different conditions: as-received, and sandblasted for 30 min and for 60 min

revealed that predamaging glass considerably lowers the dispersion of failure stress data, confirming, albeit tentatively, the conclusion that material strength does not fall below a lower bound. Another significant evidence from this work is that the difference in strength between the air side and tin side appears to vanish for predamaged glass.

Motivated by the frequent sandstorms in the Saharian regions, Madjoubi et al. (1999) analyzed the influence of sand particle impacts on glass strength. The population consisted of three sets of 50 specimens, tested in a four-point-bending configuration after a certain time  $t$  of exposure to sandblasting. One sample was tested in the pristine state  $t = 0$  and the second and the third samples were tested after a period of exposure to sandblasting of  $t = 30$  min and  $t = 60$  min, respectively. In all tests, the specimen surface was oriented perpendicular to air flow. The results are summarized in Fig. 2 in the Cartesian and Weibull planes.

It is clear that the two strength distributions, associated with  $t = 30$  min and  $t = 60$  min of sandblasting exposure time, are close to one another, but have noteworthy differences. In the pristine specimens ( $t = 0$  min), the graphs in the Weibull plane cannot be interpreted by a straight line, but instead exhibit a bilinear trend; the data associated with the lower probabilities should be

interpolated by a line whose slope is higher than the line approximating the data on the right-hand side of the graph. However, such a bimodal character is less pronounced after sandblasting. In neither case can a straight line interpolate all the data in the Weibull plane. In general, the strength diminishes after sandblasting. From the graphs of Fig. 2(b), it is noticed that for high probability of failure (high strengths), increasing the sandblasting time also reduces the strength. The opposite seems to be true at low probabilities (low strengths), when increasing the blasting time seems to have, albeit approximately, a beneficial effect on the material strengths.

Figs. 3(a and b) show representative micrographs (80 $\times$  magnification) of the surface damage induced by sand impacts after  $t = 30$  min and  $t = 60$  min, respectively. It is important to note the tendency toward a homogenization of the damage with increasing time. Fig. 4(a) shows additional details of surface erosion, including lateral cracks, nearly parallel to the surface (arrow a), cracks that extend toward and intersect the surface (arrow b), and the morphology of the scales after detachment (arrow c).

In order to confirm the effects of sandblasting on ultimate strength, in another series of tests the treatment time was increased up to 2 h. The results are summarized in Fig. 4(b), which shows the average values as well as the corresponding standard deviation.

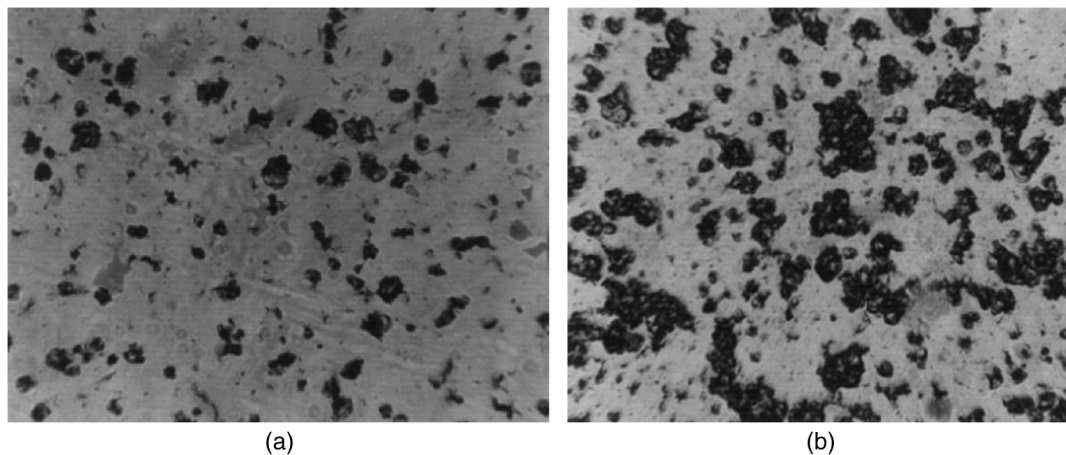


**Fig. 3.** Micrographs (82 $\times$  magnification) of the eroded surfaces, showing the damage caused by the sand particles impacts after (a) 30 min and (b) 60 min

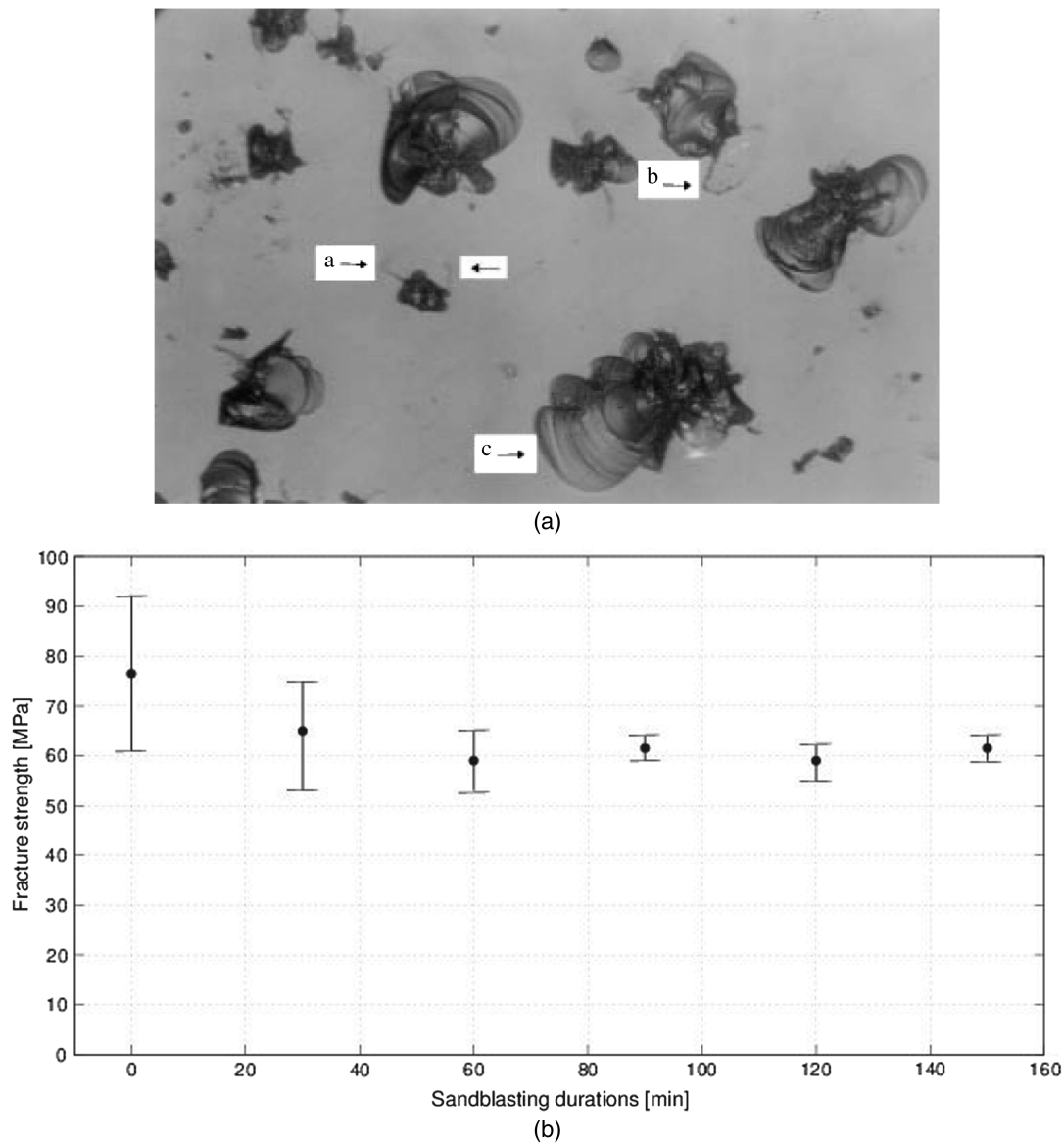


**Fig. 4.** (a) Micrographs (320 $\times$  magnification) of the damaged surfaces, showing details (arrows a, b, and c) of the formation of lateral cracks; (b) variation of the fracture strength versus sandblasting duration

From this graph, one notices a sharp drop in strength after 30 min of sandblasting, and then a nearly constant level of strength values. In fact, the strength does not decrease even after 2 h of sandblasting. The standard deviation decreases with increased sandblasting time.

Other experimental campaigns confirm these trends. Of particular interest are the tests of Pourreux (1997), assessing the strength reduction in borosilicate glass after sandblasting with round particles (Zirblast B205 powder). The measured strength was found to be a decreasing function of the kinetic energy of the impinging particles, which is evidently correlated with the amount of damage that the particles can produce on the glass surface. The fact that the macroscopic strength of glass is governed by microscopic surface defects was confirmed by further tests, where etching with hydrogen fluoride was used to chemically remove the glass layer deteriorated by the sandblasting process. Remarkably, it was demonstrated that this was a very efficient way to increase the strength of the glass structure, which was found to be an increasing function of the etching time. Indeed, micrographs of the treated specimens confirmed

that the effect of the chemical etching was that of smoothing out the glass surface, thus reducing the level of stress concentrations.

However, although the strength increased, the Weibull modulus was found to decrease with etching time. This suggests that the leveling of the existing defects was accompanied by a greater dispersion of their size and sharpness. A simulation of surface damage obtained with sandblasting was also attempted with Vickers indenters, choosing various loads in order to generate indents with (postthreshold) and without (subthreshold) radial cracks. The statistical distributions of strengths obtained by applying different forces at the indenters exhibited a transition zone. If the indent load was low, the samples behaved like nonindented ones, indicating that the intrinsic glass defects are dominant. This is confirmed by the Weibull modulus, which for this case was similar to that of the pristine glass. On the other hand, for high indent loads, the strength reduction was accompanied by a reduction of the data dispersion, determined by a higher Weibull modulus.

All the experiments lead to the tentative conclusion that the strength of glass cannot be reduced below a certain limit value

by a natural degradation process, unless the glass is specifically damaged on purpose.

### On the Possibility of a Lower Bound for Glass Strength

It is universally recognized that glass breaks due to the propagation of a dominant surface crack under positive crack opening stress. The underlying hypothesis is that the average density of the other surface flaws is such that they do not affect the fracture mechanics of the opening defect. Hence, it is natural to consider the equilibrium states of one dominant crack in a homogeneous isotropic elastic solid: rupture occurs when such a defect reaches the critical size associated with the applied stress. This is why the Weibull statistics, based upon the weakest link-in-the-chain concept, is the most widely used model for the probabilistic characterization of the mechanical resistance of glass.

As discussed in detail in the Appendix, it is reasonable to assume that the dominant crack is semicircular and its surfaces are perpendicular to the surface. Within the linear elastic fracture mechanics (LEFM) framework, if there is an upper bound  $c_{0,max}$  for the maximum radius of cracks initially present in glass, there is a lower bound for the crack opening stress that can provoke catastrophic failure. With the same notation of Eq. (55), the intrinsic lower bound for glass strength predicted by LEFM, say  $\sigma_0$ , is given by

$$\sigma_0 = \frac{K_{Ic}}{Y(\pi c_{0,max})^{0.5}} \quad (1)$$

where  $K_{Ic} = 0.75 \text{ MPa m}^{0.5}$  is the nominal fracture toughness of soda-lime glass. Therefore, the assumption of a right-skewed distribution of flaw size (upper bound for the defect size) implies that the distribution of the material strength is, on the contrary, left-skewed (lower bound for glass strength).

It should be remarked that, in general, material properties like  $K_{Ic}$ , or equivalently  $c_0$ , should be considered as random variables. This is of major importance when dealing with high-performance ceramics, whose size and, consequently, the corresponding surface flaws, are usually quite small. On the other hand, float glass plies are usually quite large, so that the distribution of surface flaws governs the response, being only marginally influenced by variation in the intrinsic material characteristics. This is why it is customary to treat the critical stress intensity factor as a deterministic value, approximately constant within the same specimen.

An upper bound for the crack size ( $c_{0,max}$ ) can be guaranteed by accurate factory production controls capable of detecting defects with absolute precision, according to which any glass with a defect exceeding this limit will be recycled in the furnaces. If this is the case,  $\sigma_0$  of Eq. (1) would represent an absolute lower bound for glass strength, associated with the worst possible condition in which the dominant crack is exactly at the right angle to direction of maximal tensile stress (Mode I opening). Any element subject to a maximum tensile stress below such limit would have the certainty of survival under instantaneous loading. However, as detailed in the Appendix, the phenomenon of subcritical crack propagation may lead to failure in time.

Several works are available in the technical literature that corroborate the hypothesis of the existence a maximum value of the preexisting flaw size in marketed glass. In particular, Yankelevsky (2014), in accordance with the prescriptions of product standards, proposed the value  $c_{0,max} = 200 \mu\text{m}$ . Nurhuda et al. (2010) argued that the maximum flaw size for large annealed glass panels is  $c_{0,max} = 278 \mu\text{m}$ . Optical analyses of the surface of glass plates indicate that the maximum size of preexisting cracks never

exceeds  $120 \mu\text{m}$  (Lindqvist and Lebet 2014), and  $100 \mu\text{m}$  following (Wereszczak et al. 2014). Of course, this limit is strongly affected by the type of production controls, handling/installing procedures, and possible further damage. Using the aforementioned values, from Eq. (1) one would obtain  $\sigma_0 = 41.95 \text{ MPa}$  for  $c_{0,max} = 200 \mu\text{m}$ , and  $\sigma_0 = 35.58 \text{ MPa}$  for  $c_{0,max} = 278 \mu\text{m}$ .

The possible existence of a lower bound for glass strength has been confirmed (Pisano and Royer-Carfagni 2015a) by the results of the statistical analysis of the experimental campaign (CEN 2006), for which the authors proposed a three-parameter Weibull distribution that naturally includes a lower bound for material strength. Data regression with this statistical model demonstrated that the lower bound is  $39 \text{ MPa}$  for the air-side data, and  $36 \text{ MPa}$  for the tin-side data, values very close to the estimates obtained from Eq. (1).

However, preexisting dominant defects could be affected by a modification of the glass surface due to corrosion and/or abrasion. The phenomenon of glass corrosion is due to the chemical aggression of alkali solutions, acids, or water. The attack of alkali solutions leads to the dissolution of the external surface, whereas acid corrosion and corrosion by water make the surface porous. The corrosion process is very gradual and creates uniformly distributed flaws that are typically much smaller than the preexisting cracks from the production process. In conclusion, recall that chemical etching produces the leveling of existing defects and, consequently, increases the glass strength (Pourreux 1997).

The flaws due to abrasion are obviously strongly affected by the cause that produces the abrasion itself. It is well known that it is easy to break glass if a sharp groove is produced by a diamond bit, but this type of artificial damage is deliberate, and cannot be associated with a natural degradation of the material. The experimental conclusions with blowing sands of Madjoubi et al. (1999) were confirmed by Wang et al. (2010), who observed that the maximum length of the long axes of the flaw caused by a 20-min exposure to sandblasting was approximately  $35 \mu\text{m}$ . Therefore, considering that sandstorms represent an extreme condition, it could be argued that the flaws due to abrasion are most likely smaller than the extremal largest cracks allowed by factory production controls. One can thus argue that the effects of aging due to abrasion are that of producing an additional uniform distribution of defects, whose depth can be considered to be less than  $200 \mu\text{m}$ .

Although the size of the dominant crack is not affected by the introduction of additional defects, all the experiments discussed herein show a decay of the lower limit for glass strength (Madjoubi et al. 1999; Durchholz et al. 1995) in abraded glass. In order to provide a qualitative explanation, observe from Figs. 3 and 4(a) that the defects induced by impinging particles resemble cavities produced on the glass surface. These can be approximated as semi-spherical, with a radius of the order of  $35\text{--}40 \mu\text{m}$  (Wang et al. 2010). Moreover, since the cavities are uniformly distributed, it is highly probable that they intersect an existing dominant crack, which can be considered to be a semicircular thumbnail crack, with a maximum radius of the order of  $100 \mu\text{m}$ .

The effect of the cavity on the stress intensity factor (SIF) distribution along the crack front can be quantified by the model problem shown in Fig. 5(a), where the cavity and the thumbnail crack have the same center. The SIFs of this configuration were calculated in Xiao and Yan (2008) by using the boundary element software *FRANC3D*. The maximum SIF in Mode I,  $K_{Im}$ , is attained at  $\phi = 0$  [same notation of Fig. 5(b)] and depends upon the ratio  $a = R/r$ . The graph of  $K_{Im}(a)$  is reported in Fig. 5(c), normalized with respect to the value  $\bar{K} = \sigma\sqrt{\pi R}$ , so that  $1.251\bar{K}$  denotes the SIF at  $\phi = 0$  for a semicircular thumbnail crack of radius  $R$ , with no interacting cavity.

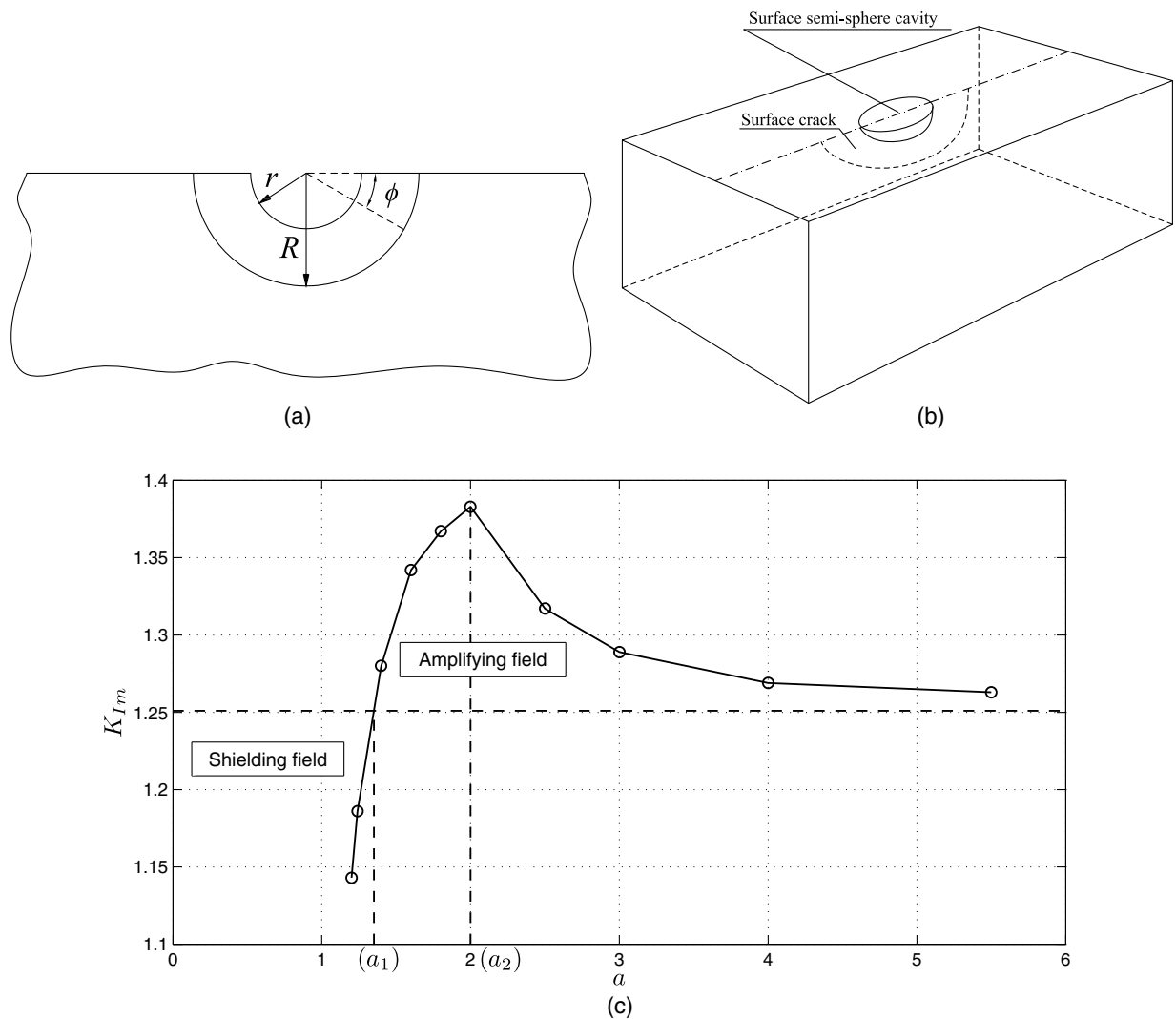


**Fig. 5.** Schematic of cracks emanating from a surface semispherical cavity in infinite elastic body: (a) total view; (b) symmetry plane in which the crack surface occurs; (c) variation of normalized SIFs with the parameter  $a = R/r$

It is observed that the cavity shields the crack when  $a < a_1 = 1.351$ , whereas its effect is an amplification when  $a > a_1 = 1.351$ . The maximum is attained when  $a = a_2 = 2$ , when the SIF increases by about 10.5%, while for  $a > a_2$  the function  $K_{I/m}(a)$  is monotonically decreasing. When  $a = 5.5$ ,  $K_{I/m}$  is 1.010 times the SIF of an isolated crack; that is, the effect of the surface cavity can be neglected. A quantitatively similar amplification from the cavity is attained at other points of the crack boundary, i.e., when  $0 < \phi \leq \pi/2$ .

This trend can justify, at least at the qualitative level, the experimental results on sandblasted glass. Referring in particular to Fig. 2, one should distinguish the part of the graphs associated with low strength and low probabilities (left-hand side) from that corresponding to high strength and high probabilities (right-hand side).

The left-hand-side extreme corresponds to specimens with the largest intrinsic defects (presumably with axis of the order of  $100 \mu\text{m}$ ), whose stress intensity factor is amplified by cavities with radius of order of  $40 \mu\text{m}$ . According to the graph of Fig. 5(c), the amplification due to the cavity diminishes if, for a fixed  $r$ , the crack size  $R$  diminishes. There is a maximum amplification at  $a = R/r = 2$  that is associated with an upper bound for the damaging action of sandblasting, for which, using Eq. (1), one would obtain a maximum reduction of the strength of the order of 10%. Going

rightwards in the graphs, the intrinsic defects in the specimens tend to become smaller ( $R$  diminishes) and, if this is the case, the amplification is reduced. This explains why the gap with the result of pristine glass also tends to become smaller. The left-hand-side tail of the graphs shows that specimens that have undergone the longer sandblasting process ( $t = 60$  min) become stronger than the others ( $t = 30$  min). This is not surprising: if increasing the time of sandblasting produces an increase in the size of the cavities and/or their number, there could certainly be a departure from the optimal value  $a = R/r = 2$ . In fact, observing Fig. 3, one realizes that if the defects become very numerous and uniformly distributed, the dominant crack could be intersected by more than one defect or the cavities may coalesce to form larger cavities, thus producing a shielding action.

The right-hand-side tail of the graphs is to be associated with the highest strength and the minimal surface damage in pristine glass. In other words, the size of the existing cracks should be much smaller than the size of the cavities produced by sandblasting. In this case, the strength of the material is no longer governed by preexisting cracks, but by the artificially produced flaws. Therefore, on the one hand, one can observe a reduction of strength, which increases by increasing the time of sandblasting. On the other hand, since the introduced flaws are uniformly distributed

and similarly sized, a reduced dispersion of the experimental data is expected. This is confirmed by the slope of the graphs in the Weibull plane that are steeper than those of the pristine specimens.

In conclusion, if one assumes the existence of a maximum characteristic size of existing flaws dictated by adequate factory production controls, there should be a lower bound for glass strength. The effects of aging, in particular natural abrasion/erosion, could further lower such a limiting stress. However, the gross strength reduction in this case would be limited because the size of the additional defects is in general smaller than the size of the maximum dominant crack. In fact, if the number of additional defects becomes large enough so that they interact with each other, they will produce a mutual shielding action.

Accepting a lower bound for glass strength represents a major change, which may be resisted as opposing the engineering sense that no structure should be assumed to be 100% safe. As showed by Pisano and Royer-Carfagni (2015a), if one uses the CEN results (CEN 2006), a limit stress of the order of 35 MPa is determined. This value was rejected by the working group CEN-TC129/WG8 because it is considered too high. The committee, therefore, decided to recommend the conservative two-parameter Weibull distribution, which has no lower bound, although the statistical analysis of Pisano and Royer-Carfagni (2015a) has demonstrated that this leads to very inaccurate interpretations of the data. To mitigate this inaccuracy, other authors (e.g., Rodichev et al. 2012) have proposed to use a bilinear Weibull distribution, i.e., to interpret the left-hand-side tail with one two-parameter Weibull distribution and the right-hand-side tail with another one. However, this approach seems to lack a sound physical justification.

Note that the lower bound that seems to emerge from the experimental data (CEN 2006) is quite high [ $\sim 35$  MPa (Pisano and Royer-Carfagni 2015a)], but if one accepts that this is due to the presence of a dominant defect, such a limit should be reduced. In particular, if the opening stress is maintained for a certain time, due to the phenomenon of subcritical crack propagation detailed in the Appendix, the crack size  $c_{0,\max}$  can increase in time according to Eq. (56). Consequently, the limit strength  $\sigma_0$  should be rescaled to the value  $\sigma_{0,\tau}$  as per Eq. (59), when the load is maintained for the time  $\tau$ . Moreover, to take into account the effects of aging, which provoke natural abrasion/erosion, it would be necessary to consider a further reduction to  $\sigma_{0,\tau}^*$ , say

$$\sigma_{0,\tau}^* = \frac{\sigma_{0,\tau}}{\omega_0} \quad (2)$$

where  $\omega_0$  = parameter that has to be specifically calibrated according to the various possible damaging actions, including those caused by handling. According to this rationale, the observed distinction in material strength between the tin and air sides should be attributed only to the presence of additional defects on the tin side from the float production process. Since the air side is the undamaged surface, the true lower bound of glass strength  $\sigma_0$  should be associated to the value measured on the air side, whereas for the tin side a reduction is expected according to Eq. (2).

### Weibull Approach and Generalized Distributions: Effects of Size, State of Stress, and Load Duration

Using the fundamental laws of probability, Weibull (1951) developed a statistical theory that is capable of interpreting the variability of the experimental data, including strength, for many materials. His weakest-link-in-the-chain-based theory relies on the assumptions that failure is the result of the collapse of one elementary material element that occurs independently of

the response of other portions of the material volume. By dividing the surface under stress into small area elements  $dA$ , the risk of rupture  $dB$  is determined by an equation of the type

$$dB = -\log(1 - P_{f,0})dA \quad (3)$$

where  $P_{f,0}$  = probability of rupture of a representative infinitesimally small element. The term  $\log(1 - P_{f,0})$  is always a negative-value function of the applied stress  $\sigma$  and so one can write  $dB = n(\sigma)dA$ , where  $n(\sigma) > 0$  is a material function that accounts for the strength properties. By considering a nonuniform distribution of stresses in the reference area  $A$ , the risk or collapse can be written as

$$B = \int_A n(\sigma)dA \quad (4)$$

Thus, defining according to Eq. (3) the overall risk of rupture as  $B = -\log(1 - P_f)$ , where  $P_f$  is the probability of rupture of the whole element, one gets

$$P_f = 1 - \exp(-B) = 1 - \exp\left[-\int n(\sigma)dA\right] \quad (5)$$

Note that the material function  $n(\sigma)$  for anisotropic materials is dependent upon the magnitude and direction of the stress, and can vary throughout the volume. On the contrary, it is a function only of the stress and position for isotropic materials.

### Two-Parameter Weibull Distribution

The two-parameter Weibull (2PW) distribution is commonly considered the best statistical model for the characterization of glass strength (Evans 1978). It is thought of as being capable of providing qualitative explanations of the variability of observed data, and it is associated with simple formulas for the mean value and standard deviation. With reference to the micromechanically motivated model of glass strength referred to in the Appendix, suppose that the state of stress is equibiaxial at each elementary portion  $dA$ , so that the principal component of tensile stress is always orthogonal to the plane of the dominant crack (Mode I opening). Freudenthal (1968) showed how to relate the flaw distribution to the Weibull strength distribution and, under very general hypotheses associated with the weakest-link-in-the-chain concept (Coleman 1958), it is possible to demonstrate that the material function has to be of the form

$$n(\sigma) = \left(\frac{\sigma}{\eta_0}\right)^m \quad (6)$$

where  $\eta_0$  and  $m$  = scale and shape parameters of the distribution, respectively. Consequently, the failure probability of a specimen (Munz and Fett 1999) is given by

$$P_{f,w2} = 1 - \exp\left[-\int_A \left(\frac{\sigma}{\eta_0}\right)^m dA\right] \quad (7)$$

The higher the  $m$ , the lower the dispersion of data.

If the state of stress is not equibiaxial, one has to take into account that only the component of stress  $\sigma_\perp$ , normal to the crack plane, has to be considered in the Mode I opening. Denoting by  $\sigma_1$  and  $\sigma_2$  the principal components of the tensile stress and with  $\psi$  the angle that the direction of  $\sigma_1$  forms with the normal to the dominant crack plane, one has

$$\sigma_\perp = [\sigma_1 \cos^2 \psi + \sigma_2 \sin^2 \psi] \quad (8)$$

It is reasonable to assume an isotropic and homogeneous distribution of defects (Franco and Royer-Carfagni 2015), i.e., there is no preferred orientation for the cracks or, equivalently, there is the same probability of finding a crack in any direction. One can thus define the equivalent value of the stress for the 2PW distribution

$$\sigma_{eq,W2} = \left[ \frac{2}{\pi} \int_0^{\pi/2} (\sigma_1 \cos^2 \psi + \sigma_2 \sin^2 \psi)^m d\psi \right] \quad (9)$$

so that the failure probability [Eq. (7)] becomes

$$P_{f,W2} = 1 - \exp \left[ - \int_A \left( \frac{\sigma_{eq,W2}}{\eta_0} \right)^m dA \right] \quad (10)$$

Moreover, denoting by  $\sigma_{max}$  the maximum tensile stress in the tensile area  $A$ , it is possible to define the *effective area* as  $A_{ef,W2} = K_{W2}A$ , synthetically accounting for the influence of the size and the stress state upon the probability of failure (Choi et al. 2000), according to the equivalence

$$1 - \exp \left[ - \int_A \left( \frac{\sigma_{eq,W2}}{\eta_0} \right)^m dA \right] = 1 - \exp \left[ - K_{W2}A \left( \frac{\sigma_{max}}{\eta_0} \right)^m \right] \quad (11)$$

so that

$$A_{ef,W2} = K_{W2}A = \frac{\int_A (\sigma_{eq,W2})^m dA}{(\sigma_{max})^m} \quad (12)$$

Obviously, in a uniform equibiaxial state of stress ( $\sigma_1 = \sigma_2 = \sigma_{max,eqb}$ ), then  $\sigma_{eq,W2} = \sigma_{max,eqb}$  and, from Eq. (12),  $K_{W2} = 1$ , so that

$$P_{f,W2} = 1 - \exp \left[ - \int_A \left( \frac{\sigma_{max,eqb}}{\eta_0} \right)^m dA \right] \quad (13)$$

In general  $K_{W2} < 1$ , which means that a specimen under a generic stress state has a lower probability of failure than under an equibiaxial state. This is why the equibiaxial stress state is generally accepted as the reference state for the characterization of the material strength. Moreover, since results are size dependent, it is customary to assume as the reference size the unitary area  $A_u = 1 \text{ m}^2$ .

Within the aforementioned approach, it is then possible to rescale the population of results obtained from a particular test configuration toward the configuration of uniformly distributed equibiaxial stress ( $\sigma_{eqb,A_u,W2}$ ) acting on a unitary ( $1 \text{ m}^2$ ) area  $A_u$ . For specimens with identical distributions of defects, by using a criterion of equal failure probability, from Eq. (11) one can write

$$\left[ -A_u \left( \frac{\sigma_{eqb,A_u,W2}}{\eta_0} \right)^m \right] = \left[ -K_{W2}A \left( \frac{\sigma_{max}}{\eta_0} \right)^m \right] \quad (14)$$

which leads to

$$\sigma_{eqb,A_u,W2} = \sigma_{max} \left( \frac{K_{W2}A}{A_u} \right)^{1/m} \quad (15)$$

It is important to remark that the aforementioned rescaling depends upon the assumed 2PW distribution for the population of material strengths.

### Three-Parameter Weibull Distribution

If the material in itself has an intrinsic lower ultimate strength  $\sigma_0$ , Weibull proposed to use a material function of the type

$$n(\sigma) = \left( \frac{\sigma - \sigma_0}{\eta_0} \right)^m \quad (16)$$

which is defined only when  $\sigma \geq \sigma_0$ . The probability of failure  $P_f$  is interpreted by a three-parameter Weibull (3PW) distribution of the type

$$P_{f,W3} = 1 - \exp \left[ - \int_A \left( \frac{\sigma - \sigma_0}{\eta_0} \right)^m dA \right] \quad (17)$$

where again,  $\eta_0$  and  $m$  = scale and shape parameter of the distribution while  $\sigma_0$  is the location parameter indicating the lower bound. This model for glass strength is consistent with the experimental evidence discussed earlier.

When the state of stress is not equibiaxial, one should define the equivalent stress  $\sigma_{eq,W3}$  similarly to Eq. (9); however, the situation is more complicated because of the lower bound  $\sigma_0$ . Denoting again with  $\sigma_1$  and  $\sigma_2$  the principal components of stress and with  $\psi$  the angle formed by the normal to the crack plane and the principal direction of  $\sigma_1$ , the crack opening stress in Mode I is again given by Eq. (8). Then, denoting with  $|\cdot|^+$  the positive part of the quantity in brackets, one can assume the expression

$$\sigma_{eq,W3} - \sigma_0 = \frac{2}{\pi} \int_0^{\pi/2} (|\sigma_1 - \sigma_0|^+ \cos^2 \psi + |\sigma_2 - \sigma_0|^+ \sin^2 \psi) d\psi \quad (18)$$

This means that glass is sensitive only to those tensile stresses that exceed  $\sigma_0$ . In fact,  $P_f = 0$  if and only if  $\sigma_1 \leq \sigma_0$  and  $\sigma_2 \leq \sigma_0$ .

It is worth mentioning that a slightly different expression for  $\sigma_{eq,W3}$  had been proposed in Pisano and Royer-Carfagni (2015a), formula (4.13), i.e.

$$\sigma_{eq,W3} - \sigma_0 = \frac{1}{\pi} \int_0^{\pi} |\sigma_1 \cos^2 \psi + \sigma_2 \sin^2 \psi - \sigma_0|^+ d\psi \quad (19)$$

but this assumption is not conservative because it implies that only the spatial average of the stress has to be compared with the lower bound  $\sigma_0$ ; consequently, there could be states of stress with, say,  $\sigma_1 > \sigma_0$  and  $\sigma_2 < \sigma_0$ , that are always safe.

Consequently, the probability of failure for the whole specimen becomes

$$P_{f,W3} = 1 - \exp \left[ - \int_A \left( \frac{\sigma_{eq,W3} - \sigma_0}{\eta_0} \right)^m dA \right] \quad (20)$$

Introducing the effective area  $A_{ef,W3} = K_{W3}A$ , this expression could be rewritten as

$$P_{f,W3} = 1 - \exp \left[ - A_{ef,W3} \left( \frac{\sigma_{max} - \sigma_0}{\eta_0} \right)^m \right] \quad (21)$$

where

$$A_{ef,W3} = K_{W3}A = \frac{\int_A (\sigma_{eq,W3} - \sigma_0)^m dA}{(\sigma_{max} - \sigma_0)^m} \quad (22)$$

Clearly,  $K_{W3} \leq 1$  and  $K_{W3} = 1$  if and only if the state of stress is uniformly equibiaxial and higher than  $\sigma_0$ .

Moreover, equating the failure probabilities so that

$$\begin{aligned} 1 - \exp \left[ - A_u \left( \frac{\sigma_{eqb,A_u,W3} - \sigma_0}{\eta_0} \right)^m \right] \\ = 1 - \exp \left[ - A_{ef,W3} \left( \frac{\sigma_{max} - \sigma_0}{\eta_0} \right)^m \right] \end{aligned} \quad (23)$$

one can find the equivalent uniform equibiaxial stress ( $\sigma_{eqb.A_u.W3}$ ) acting on the unitary area ( $A_u = 1 \text{ m}^2$ ) in the form

$$\sigma_{eqb.A_u.W3} = \sigma_{\max} \left( \frac{A_{ef.W3}}{A_u} \right)^{1/m} - \sigma_0 \left[ \left( \frac{A_{ef.W3}}{A_u} \right)^{1/m} - 1 \right] \quad (24)$$

From the discussion about the possibility of a lower bound for glass strength, the quantity  $\sigma_0$  should be associated with the maximum size of defects that can be found on the glass surface. However, one has to take into account the phenomenon of static fatigue. Starting from Eq. (56), one can reach an expression like Eq. (59) that correlates the opening stress  $\sigma_{0,\tau}$  that provokes failure if constantly applied for the time  $\tau$ , with the opening stress  $\sigma_0$  that provokes failure during a test in lab at a constant stress rate  $\dot{\sigma}$  (most standards suggest to use  $\dot{\sigma} = 2 \text{ MPa/s}$ ). Reasoning as in Appendix, one obtains the expression

$$\sigma_{0,\tau} = \frac{(\sigma_0)^{(n+1)/n}}{[(n+1)\tau\dot{\sigma}]^{1/n}} \quad (25)$$

One can estimate  $\sigma_0$  from the regression of experimental data from tests performed at the constant stress rate  $\dot{\sigma}$ , using for example the results of the experimental campaign (CEN 2006), where  $\dot{\sigma} = 2 \text{ MPa}$ . Rigorously speaking, for each experimental datum it would be necessary to make a rescaling as per Eq. (25) according to the time that is necessary to provoke rupture. In other words, the value of  $\sigma_0$  obtained from the experimental data regression has an intrinsic dependence upon the time that has been necessary to provoke rupture. This is different from the value of  $\sigma_0$ , obtained from Eq. (1), which instead refers to instantaneous rupture.

Finally, it worth remarking that in the 3PW approach the lower bound for glass strength clearly does not depend upon the size of the specimen because it is associated with the worst possible condition in terms of defect location and state of stress. Indeed, it should be interpreted here as an absolute limit that attains the same value for specimens of any geometry.

### Left-Truncated Weibull Distribution

The left-truncated Weibull (LTW) distribution, as the 3PW, provides a lower bound value of the strength. Even though the two distributions may appear similar, the interpretation of the lower limit is very different. In fact, whereas according to the 3PW the location parameter  $\sigma_0$  is considered an intrinsic limit of the statistical population, the lower limit given by the LTW distribution is the result of a truncation of the population of experimental data.

Following Weibull (1939), let  $P_f(\sigma)$  represent the probability of failure at stress  $\sigma$  of the population, evaluated following a certain prescribed test, and  $B(\sigma)$  the corresponding risk of failure, with  $B = -\log(1 - P_f)$ . Then, suppose that with a factory production control, all those test specimens whose ultimate strength is less than  $\sigma_0$  are eliminated. If the stress  $\sigma_0$  corresponds to the probability  $P_0$ , and if the original number of specimens is  $N$ , then the number of specimens remaining after the elimination will be  $N(1 - P_0)$ . One can thus obtain the (truncated) probability of failure for the remaining population of specimens  $P_f^T(\sigma)$  as

$$P_f^T(\sigma) = \frac{[P_f(\sigma) - P_0]N}{(1 - P_0)N} = 1 - \frac{1}{1 - P_0} \exp[-B(\sigma)], \quad \text{for } \sigma > \sigma_0 \quad (26)$$

where  $P_0 = \text{constant}$ . Since  $P_f^T(\sigma_0) = 0$ , one assumes that  $1 - P_0 = \exp(-B(\sigma_0))$ , and consequently from Eq. (27) one finds

$$P_f^T(\sigma) = 1 - \exp\{-[B(\sigma) - B(\sigma_0)]\}, \quad \text{for } \sigma > \sigma_0 \quad (27)$$

By assuming that the parent distribution of glass strengths is a 2PW distribution, then Eq. (6) holds, and from Eq. (4) one obtains

$$P_{f.WT} = 1 - \exp\left[-\frac{\int_A (\sigma^m - \sigma_0^m) dA}{\eta_0^m}\right] \quad (28)$$

Such an expression holds for equibiaxial stress states. For a general type of stress, one can define the equivalent stress  $\sigma_{eq.WT}$ , which takes a form identical to Eq. (9). In conclusion, the probability of failure becomes

$$\begin{aligned} P_{f.WT} &= 1 - \exp\left[-\frac{\int_A (\sigma_{eq.WT}^m - \sigma_0^m) dA}{\eta_0^m}\right] \\ &= 1 - \exp\left[-\frac{K_{WT}\sigma_{\max}^m - \sigma_0^m}{\eta_0^m} A\right] \end{aligned} \quad (29)$$

where  $K_{WT}$  = correction coefficient for the effective area of the left-truncated distribution, which reads

$$K_{WT} = \frac{\int_A \sigma_{eq.WT}^m dA}{A\sigma_{\max}^m} \quad (30)$$

For what concerns the rescaling toward the standard reference conditions (uniform equibiaxial stress  $\sigma_{eqb.A_u.WT}$  on the unitary area  $A_u = 1 \text{ m}^2$ ), equal failure probability is obtained provided that

$$1 - \exp\left[-\frac{K_{WT}\sigma_{\max}^m - \sigma_0^m}{\eta_0^m} A\right] = 1 - \exp\left[-\frac{\sigma_{eqb.A_u.WT}^m - \sigma_0^m}{\eta_0^m} A_u\right] \quad (31)$$

which provides the stress rescaling

$$\sigma_{eqb.A_u.WT} = \left[ \frac{K_{WT}A\sigma_{\max}^m}{A_u} - \sigma_0^m \frac{(A - A_u)}{A_u} \right]^{1/m} \quad (32)$$

Comparing the 3PW distribution of Eq. (20) or Eq. (21) with the LTW distribution of Eq. (29) shows that both present the lower bound  $\sigma_0$  for glass strength. But whereas in the 3PW case this represents an intrinsic material limit, in the LTW the value  $\sigma_0$  is obtained from the elimination of some data from a given population. In other words, in the LTW case the limit  $\sigma_0$  is associated with the population of data itself and, implicitly, with the particular testing procedure that has been employed to obtain such a population. If the testing procedure is varied, the data change and one obtains a new population. It is thus not surprising that the specimens to be eliminated should be associated with a different value of the left truncation. More specifically, from Eq. (29) it is clear that the lower bound becomes  $\sigma_0(K_{WT})^{-1/m}$ , i.e., it depends on the type of stress that is induced in the specimen. However, since as an order of magnitude  $m \approx 6$  for float glass, even for a very small value  $K_{WT} \approx 0.3$ , one would obtain an increase of the order of 20%.

The usefulness of the LTW distribution is that it provides significant analytical simplifications as compared with the 3PW function. Specifically, for the 3PW case the definition in Eq. (18) implies that the state of stress is everywhere multiplied by the given constant. Thus, there is a strongly nonlinear dependence upon such a constant for what the equivalent stress  $\sigma_{eq.W3}$  is concerned. This implies that the effective area  $A_{ef.W3}$  of Eq. (22) must be calculated for all stress conditions. For the LTW, on the other hand, the definition of the equivalent stress  $\sigma_{eq.WT}$ , analogous to Eq. (9), is a linear function of the stress state. Consequently, during a test where the load is homogeneously increased, if one neglects

geometric second-order effects, the correction coefficient  $K_{WT}$  of Eq. (30) would be independent of  $\sigma_{\max}$ .

In conclusion, the physical significance of the collocation parameter  $\sigma_0$  for the 3PW and the the LTW distributions is quite similar, but whereas in the first case it is an intrinsic material property, in the second case it is associated with a particular production control that allows to eliminate the bad specimens. The meaning of bad is associated with the particular type of production control that is employed. For both cases, the value of  $\sigma_0$  is associated with the maximum size of the pre-existing defects in the glass specimen. Because of the phenomenon of subcritical crack propagation, it has to be rescaled for the LTW to account for loading time as it was for the 3PW case according to Eq. (25).

### Weibull Distributions without a Lower Bound

As discussed earlier, Fig. 1 makes it clear that the data on the Weibull plane does not lie on a straight line as dictated by the 2PW distribution. However, the presence of a lower bound for glass strength is not always accepted by many engineers and researchers, who have preferred to interpolate the observed measurements with a generalized two-parameter Weibull distributions that does not have a limit on the left-hand-side tail.

### Bilinear Weibull Distribution

The simplest idea consists in interpolating the experimental points with a piecewise linear function, as proposed by Rodichev et al. (2012). However, the approach is not without ambiguity if one consider that the state of stress inside the material is in general not uniformly equibiaxial. This can be illustrated by defining the equivalent stress  $\sigma_{eq,WB}$  through an expression identical to that of Eq. (9) for the 2PW distribution. In the simplest case, one can assume a bilinear function for the Weibull distribution (BLW) of the form

$$P_{f,WL} = \begin{cases} 1 - \exp \left[ - \int_A \left( \frac{\sigma_{eq,WL}}{\eta_1} \right)^{m_1} dA \right], & \text{for } 0 < \sigma_{\max} \leq \sigma^* \\ 1 - \exp \left[ - \int_A \left( \frac{\sigma_{eq,WL}}{\eta_2} \right)^{m_2} dA \right], & \text{for } \sigma_{\max} > \sigma^* \end{cases} \quad (33)$$

where  $(\eta_1, m_1)$  and  $(\eta_2, m_2) = 2PW$  coefficients corresponding to the left-hand-side and right-hand-side branches, respectively, while  $\sigma_{\max}$  is the maximum stress for the element under consideration. Notice that in this approach the choice of the Weibull coefficients is made upon the stress  $\sigma_{\max}$ . Another approach would be to consider the distribution

$$\hat{P}_{f,WL} = 1 - \exp \left\{ - \int_A \left[ \frac{\sigma_{eq,WL}}{\eta(\sigma_{eq,WL})} \right]^{m(\sigma_{eq,WL})} dA \right\} \quad (34)$$

where

$$[\eta(\sigma_{eq,WL}), m(\sigma_{eq,WL})] \begin{cases} (\eta_1, m_1) & \text{for } 0 < \sigma_{eq,WL} \leq \sigma^* \\ (\eta_2, m_2) & \text{for } \sigma_{eq,WL} > \sigma^* \end{cases} \quad (35)$$

but such a choice would lead to serious complications, because one would have to change the Weibull parameters within the same structural element.

If one assumes Eq. (33) is analogous to Eq. (12), one can introduce the effective area  $A_{ef,WL} = K_{WL}A$ , that for this specific case can be written as

$$A_{ef,WL} = K_{WL}A = \begin{cases} \frac{\int_A (\sigma_{eq,WL})^{m_1} dA}{(\sigma_{\max})^{m_1}} & \text{for } 0 < \sigma_{\max} \leq \sigma^* \\ \frac{\int_A (\sigma_{eq,WL})^{m_2} dA}{(\sigma_{\max})^{m_2}} & \text{for } \sigma_{\max} > \sigma^* \end{cases} \quad (36)$$

On the other hand, under the hypothesis that Eq. (34) holds, one would find the much more complicated expression

$$\hat{A}_{ed,WL} = \hat{K}_{WL}A = \begin{cases} \left( \frac{\eta_1}{\sigma_{\max}} \right)^{m_1} \int_A \left[ \frac{\sigma_{eq,WL}}{\eta(\sigma_{eq,WL})} \right]^{m(\sigma_{eq,WL})} dA, & \text{for } 0 < \sigma_{\max} \leq \sigma^* \\ \left( \frac{\eta_2}{\sigma_{\max}} \right)^{m_2} \int_A \left[ \frac{\sigma_{eq,WL}}{\eta(\sigma_{eq,WL})} \right]^{m(\sigma_{eq,WL})} dA, & \text{for } \sigma_{\max} > \sigma^* \end{cases} \quad (37)$$

where  $\eta(\sigma_{eq,WL})$  and  $m(\sigma_{eq,WL})$  are defined as in Eq. (35).

Rescaling of the experimental data obtained in the particular test configuration toward standard conditions (uniformly equi-biaxial state of stress, say  $\sigma_{eqb,A_u,WL}$ , acting on the unitary area  $A_u = 1 \text{ m}^2$ ) is not straightforward as in Eq. (14), because one has to choose which one of the pairs  $(\eta_1, m_1)$  or  $(\eta_2, m_2)$  to select according to the values of  $\sigma_{eqb,A_u,WL}$ . This choice is quite arbitrary since to the authors' knowledge, apart from the heuristic explanations set forth in the following, the bilinear Weibull statistics does not seem to be corroborated by any physical model. There is no need to remark further that the piecewise-linear distribution becomes extremely complicated if more than two Weibull pairs are chosen to interpolate the results.

### Bimodal Weibull Distribution

In order to obtain a smooth transition between the data interpolated with two Weibull distributions (bimodal Weibull, or BMW), one can assume that the material has undergone two distinguished and independent failure mechanisms, each one governed by a specific Weibull distribution of the type in Eq. (10), with corresponding parameters  $(\eta_1, m_1)$  and  $(\eta_2, m_2)$ . In the weakest-link-in-the-chain rationale, this is equivalent to assume that the chain consists of two types of rings, as schematically represented in Fig. 6(a).

One can thus assume that the probability of survival of the system is the product of the probability of survival of the two constituent types of chain rings. Defining the equivalent stress  $\sigma_{eq,WL}$  as per Eq. (9), then the corresponding cumulative probability distribution of failure reads

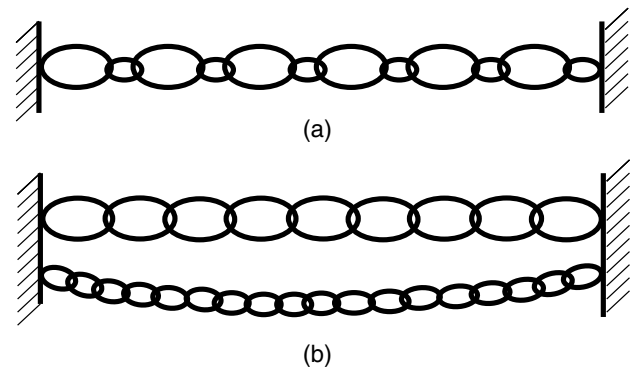


Fig. 6. (a) Bimodal chain, formed by two types of rings; (b) consecutive-loss-of-strength chain concept

$$\begin{aligned} \check{P}_{f,WM} &= 1 - \exp \left[ - \int_A \left( \frac{\sigma_{eq,WM}}{\eta_1} \right)^{m_1} dA \right] \exp \left[ - \int_A \left( \frac{\sigma_{eq,WM}}{\eta_2} \right)^{m_2} dA \right] \\ &= 1 - \exp \left\{ \int_A - \left[ \left( \frac{\sigma_{eq,WM}}{\eta_1} \right)^{m_1} + \left( \frac{\sigma_{eq,WM}}{\eta_2} \right)^{m_2} \right] dA \right\} \quad (38) \end{aligned}$$

However, in the Weibull plane one would obtain a graph whose slope is higher on the right-hand-side tail than on the left-hand-side tail, that is, the contrary of what one would expect to fit the experimental data (Fig. 1). In order to obtain the desired trend, one should assume a cumulative probability of failure, which is the product of the cumulative probabilities of failures for each constituent set of rings, i.e.

$$\begin{aligned} \hat{P}_{f,WM} &= \left\{ 1 - \exp \left[ - \int_A \left( \frac{\sigma_{eq,WM}}{\eta_1} \right)^{m_1} dA \right] \right\} \\ &\quad \times \left\{ 1 - \exp \left[ - \int_A \left( \frac{\sigma_{eq,WM}}{\eta_2} \right)^{m_2} dA \right] \right\} \\ &= 1 - \exp \left[ - \int_A \left( \frac{\sigma_{eq,WM}}{\eta_1} \right)^{m_1} dA \right] \\ &\quad - \exp \left[ - \int_A \left( \frac{\sigma_{eq,WM}}{\eta_2} \right)^{m_2} dA \right] \\ &\quad + \exp \left\{ \int_A - \left[ \left( \frac{\sigma_{eq,WM}}{\eta_1} \right)^{m_1} + \left( \frac{\sigma_{eq,WM}}{\eta_2} \right)^{m_2} \right] dA \right\} \quad (39) \end{aligned}$$

A physical justification of Eq. (52) is less straightforward. One may rely upon the schematic of Fig. 6(b), where one of the chains is taut while the other is loose. If the lateral supports are pulled apart, one has to break the first chain before the second one becomes engaged and in turn breaks. The probability of failure of the system at a certain stress level is equal to the probability that both chains break at that level, so that Eq. (52) is obtained. However, it is difficult to figure out such a scenario in a real system because it would imply the activation of two consecutive failure mechanisms, independent of one another.

Similarly to Eq. (12), one can define the effective area  $\check{A}_{ef,WM} = \check{K}_{WM}A$  that, taking into account Eq. (38), needs to satisfy

$$\begin{aligned} \check{A}_{ef,WM} &\left[ \left( \frac{\sigma_{max}}{\eta_1} \right)^{m_1} + \left( \frac{\sigma_{max}}{\eta_2} \right)^{m_2} \right] \\ &= \int_A \left[ \left( \frac{\sigma_{eq,WM}}{\eta_1} \right)^{m_1} + \left( \frac{\sigma_{eq,WM}}{\eta_2} \right)^{m_2} \right] dA \quad (40) \end{aligned}$$

An analogous expression is obtained for  $\hat{A}_{ef,WM} = \hat{K}_{WM}A$  by using Eq. (52). The result is extremely complicated.

Rescaling toward the experimental condition of uniformly equi-biaxial state of stress  $\sigma_{eqb,A_u,WM}$ , acting on the unitary area ( $A_u = 1 \text{ m}^2$ ) is again extremely difficult as in the case of the bilinear Weibull model.

### Extended Weibull Distribution

The major difficulty with the BLW and BMW models is that the presence of two Weibull exponents renders any rescaling extremely difficult. This is why many authors have attempted to define distributions that are more flexible in modeling lifetime data, but retain one Weibull exponent. In particular, Marshall and Olkin (1997) proposed a new method for adding a parameter to a family of distributions, whose application for the Weibull families can be expressed as

$$P_{f,WE} = 1 - \frac{\nu \tilde{P}_s}{1 - (1 - \nu) \tilde{P}_s} \quad (41)$$

where

$$\tilde{P} = \exp \left[ - \int_A \left( \frac{\sigma_{eq,WE}}{\eta_0} \right)^m dA \right] \quad (42)$$

and the equivalent stress  $\sigma_{eq,WE}$  takes again the same form of Eq. (9).

In order to define the effective area  $A_{ef,WE} = K_{WE}A$ , one has to satisfy the equality

$$\begin{aligned} 1 - \frac{\nu \exp \left[ -K_{WE}A \left( \frac{\sigma_{max}}{\eta_0} \right)^m \right]}{1 - (1 - \nu) \exp \left[ -K_{WE}A \left( \frac{\sigma_{max}}{\eta_0} \right)^m \right]} \\ = 1 - \frac{\nu \exp \left[ \int_A \left( \frac{\sigma_{max}}{\eta_0} \right)^m dA \right]}{1 - (1 - \nu) \exp \left[ \int_A \left( \frac{\sigma_{max}}{\eta_0} \right)^m dA \right]} \quad (43) \end{aligned}$$

from which one finds that  $A_{ef,WE} = A_{ef,W2}$  and  $K_{W2} = K_{WE}$  as per Eq. (12). Thus, the effective area takes the same form of the two-parameter Weibull distribution. In an analogous manner, one can rescale the experimental data toward the uniform equibiaxial stress  $\sigma_{eq,A_u,WE}$  acting on the unitary area  $A_u$  by setting

$$\begin{aligned} 1 - \frac{\nu \exp \left[ -A_u \left( \frac{\sigma_{eq,A_u,WE}}{\eta_0} \right)^m \right]}{1 - (1 - \nu) \exp \left[ -A_u \left( \frac{\sigma_{eq,A_u,WE}}{\eta_0} \right)^m \right]} \\ = 1 - \frac{\nu \exp \left[ -K_{WE}A \left( \frac{\sigma_{max}}{\eta_0} \right)^m \right]}{1 - (1 - \nu) \exp \left[ -K_{WE}A \left( \frac{\sigma_{max}}{\eta_0} \right)^m \right]} \quad (44) \end{aligned}$$

so as to obtain

$$\sigma_{eq,A_u,WE} = \sigma_{eq,A_u,W2} = \sigma_{max} \left( \frac{K_{WE}A}{A_u} \right)^m \quad (45)$$

Therefore, the rescaling takes exactly the same form as that of the two-parameter Weibull distribution of Eq. (15).

Although this distribution provides a very simple formulation, its major drawback is that the left-hand-side and right-hand-side tails are supposed to present the same slope in the Weibull plane (Zhang and Xie 2007). Observing the data in Fig. 1 for the air-side of the glass, one can notice that, albeit quite weakly, the probability tends to increase as  $\sigma \rightarrow \infty$ , so that the slope of an interpolating curve at the very right-hand-side extremity would tend to fit with the slope associated with very low probabilities ( $\sigma \rightarrow 0$ ). The bulk of the data should, therefore, be associated with the transition zone of the extended Weibull (EXW) distribution, so that calibration is not straightforward (Hirose 2002). However, the same asymptotical properties for  $\sigma \rightarrow 0$  and  $\sigma \rightarrow \infty$  are not so evident when the tin-side data of Fig. 1 are considered, or for the data recorded in Fig. 2.

### Experimental Confirmations

To the authors' knowledge, the only experimental program that provides sufficient data for statistical analysis is the one produced by working group CEN/TC129-WG8, which is comprised of 741 measurements (CEN 2006). Other campaigns have produced limited number of data points that are not made available in the literature. Therefore, assessment of the proposed statistical models relies on comparisons with the aforementioned data.

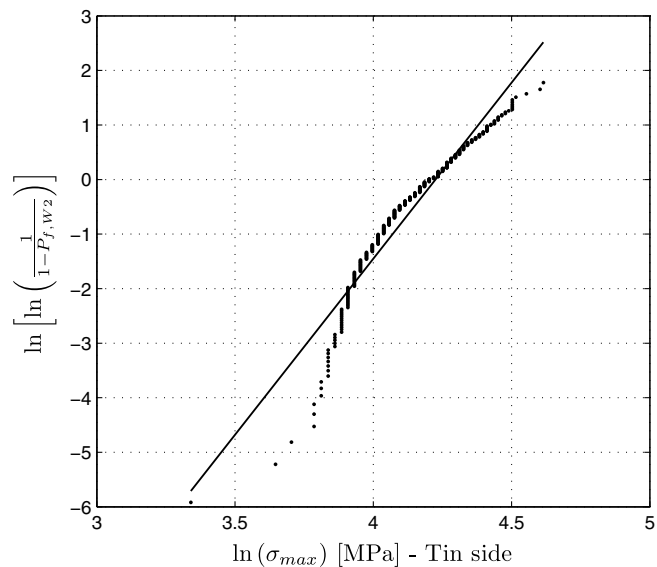
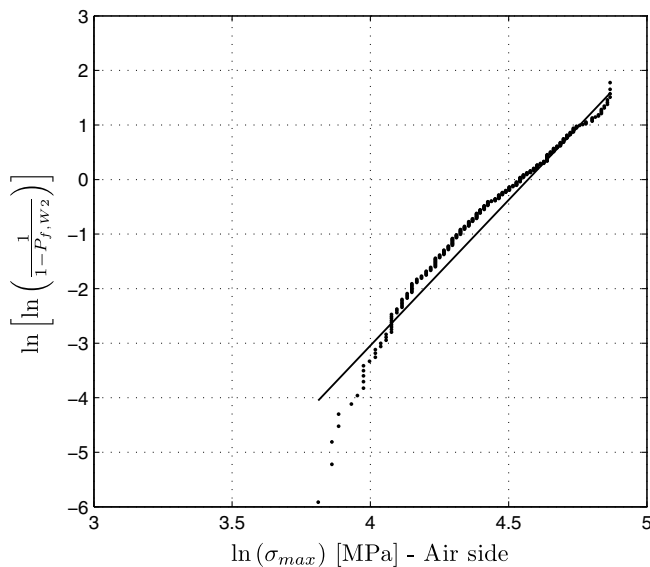


**Fig. 7.** Linear interpolation in the two-parameter Weibull plane of the failure stress measurements by CEN/TC129/WG8; distinction between tin- and air-side measurements

### Data Regression and the Two-Parameter Weibull Distribution

The Weibull parameters are usually determined through a graphically based regression of the experimental data. The measured failure stress values  $\sigma_i$  are ranked in ascending order and a failure probability  $P_i$  is assigned to each of them according to a probability estimator. The most commonly used probability estimators are

$$P_i = \frac{i}{n+1}, \quad P_i = \frac{i-0.5}{n}, \quad \text{or} \quad P_i = \frac{i-0.3}{n+0.4} \quad (46)$$

where  $n$  = total number of data. Here, the first of these is selected because it provides the most conservative results for the 2PW modulus and is, therefore, the most frequently used for design purposes.

The 2PW probability plot is obtained by the equation for the probability of failure [Eq. (10)], but since the data report the  $\sigma_{\max}$  in the specimen, it is useful to use the notion of effective area  $A_{ef,W2} = K_{W2}A$  as per Eq. (12) and apply the alternative form established by Eq. (11). One can thus write

$$P_{f,W2} = 1 - \exp \left[ - \left( \frac{\sigma_{\max}}{\eta_0 / A_{ef,W2}^{1/m}} \right)^m \right] \\ \Rightarrow \ln \left[ \ln \left( \frac{1}{1 - P_{f,W2}} \right) \right] = m \ln(\sigma_{\max}) - m \ln(\eta_0 / A_{ef,W2}^{1/m}) \quad (47)$$

where  $\sigma_{\max}$  = maximum tensile stress measured in the specimen, while  $m$  and  $\eta_0$  = shape and scale parameter, respectively.

In general, the quantity  $A_{ef,W2}$  depends upon the state of stress in the specimen, as prescribed by Eq. (12). However, if a linear elastic model is used, there is a linear correspondence between  $\sigma_{eq,W2}$  and  $\sigma_{\max}$  and the dependence is lost. In other words, there is a variation of  $A_{ef,W2}$  only if the testing procedure involves non-linear geometric effects. These can be of importance (Pisano and Royer-Carfagni 2015b) for the test method (CEN/TC129 2001a), but can be neglected, at least as a first-order approximation. Under

this hypothesis, if the experimental data are plotted in the Weibull plane, with axes  $\ln \ln 1/(1 - P_f)$  and  $\ln \sigma$ , they should be aligned.

There are various methods to find the optimal Weibull parameters. The graphical approach consists in fitting the line of Eq. (47) to the data using the least-square method. Another very used method is the maximum likelihood parameter estimation (MLE) (Cohen 1965), but its application presents difficulties for generalized distributions with more than two parameters. For all the cases considered in this article, the authors have used the graphical approach. The plots corresponding to the 2PW statistics, distinguished for the tin and air side, are shown in Fig. 7.

Recall that the experimental points recorded in CEN (2001a) had to be corrected in order to fix a systematic error contained in a calibration graph of the standard (CEN 2001a). However, as already discussed at length (Pisano and Royer-Carfagni 2015a), the approximation given by the 2PW statistics is very poor, both for the air- and the tin-side data.

### Weibull Distributions with a Lower Bound

For the three-parameter Weibull model, one can use Eq. (21), where the effective area  $A_{ef,W3} = K_{W3}A$  is defined by Eq. (22), leading to

$$P_{f,W3} = 1 - \exp \left[ - \left( \frac{\sigma_{\max} - \sigma_0}{\eta_0 / A_{ef,W3}^{1/m}} \right)^m \right] \\ \Rightarrow \ln \left[ \ln \left( \frac{1}{1 - P_{f,W3}} \right) \right] = m \ln(\sigma_{\max} - \sigma_0) - \ln(\eta_0^m / A_{ef,W3}) \quad (48)$$

One can set  $y = \ln \ln 1/(1 - P_f)$ ,  $x = \ln(\sigma - \sigma_0)$ , and  $B = -\ln(\eta_0^m / A_{ef,W3})$ . Consequently, the value of the location parameter  $\sigma_0$  might be selected by requiring that the data in the 3PW plane,  $\ln \ln 1/(1 - P_f)$  versus  $\ln(\sigma - \sigma_0)$ , are as much as possible aligned. From the interpolating line  $y = mx + B$ , one can obtain the Weibull parameters from comparison with Eq. (48). However, apart from the error that may be introduced using the aforementioned graphical method, one should recall from Eq. (22) that (even if a linear elastic approach is used and second-order effects are

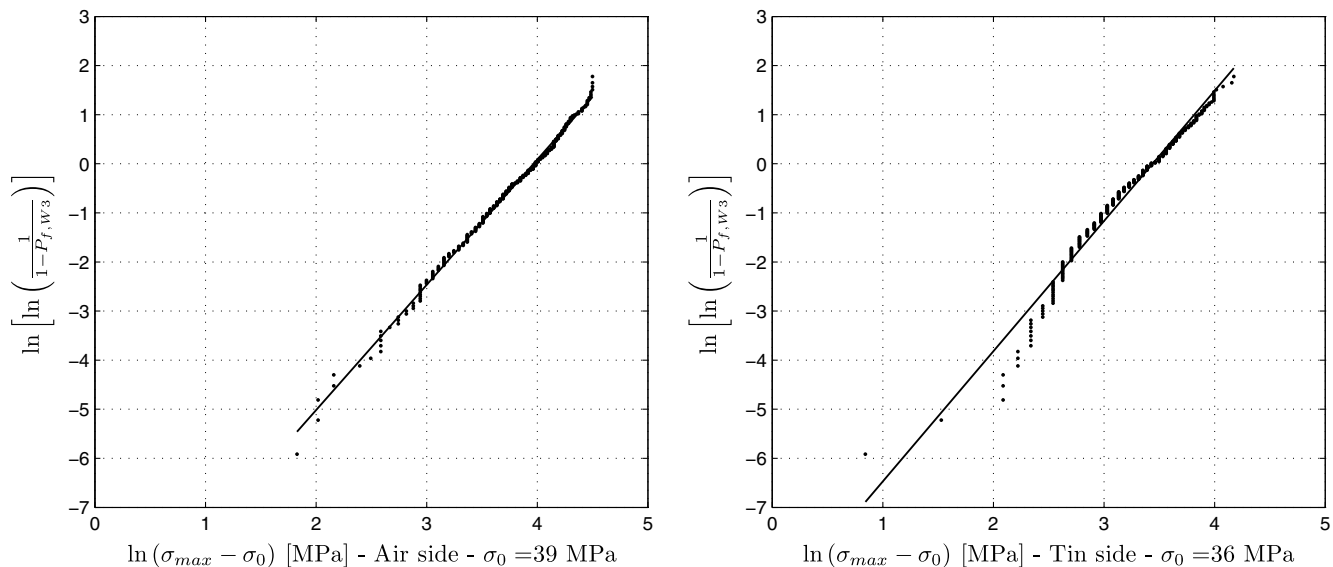


**Fig. 8.** Linear interpolation in the three-parameter Weibull plane  $\ln \ln 1/(1 - P_f)$  versus  $\ln(\sigma - \sigma_0)$  of the failure stress measurements by CEN/TC129/WG8; distinction between tin-side and air-side measurements

neglected) there is not a linear correspondence between  $(\sigma_{eq,W3} - \sigma_0)$  and  $(\sigma_{max} - \sigma_0)$ . Thus, in general,  $A_{ef,W3}$  depends upon  $\sigma_{max}$  and the dependence is more pronounced if one uses Eq. (18), rather than Eq. (19), for the estimation of the equivalent stress  $\sigma_{eq,W3}$ .

Therefore, the exact calibration of the 3WP statistics requires a more complex iterative procedure, where one tentatively chooses the shape parameter  $m$ , calculates  $A_{ef,W3}$  according to Eq. (22), then attempts the best graphical representation to find the collocation parameter  $\sigma_0$  from best alignment of the data, and finally finds  $m$  from linear interpolation. The procedure is repeated up to convergence. However, observing that in Eq. (48) the quantity  $A_{ef,W3}$  is elevated to the  $1/m$  power and that  $m$  is in general of the order of  $5/7$ , even if  $A_{ef,W3}$  is doubled, its power increases of  $10/15\%$ . Therefore, here such a dependence can be neglected.

The corresponding results are shown in Fig. 8. At first sight, it is observed that an excellent linear fit can be obtained for the air-side data, but the approximation is not as good for the tin-side data. The slope of the interpolating line is the value of  $m$ , whereas from the estimation of  $B$ , i.e., the point where the line intercepts the  $y$  axis, one finds  $\eta_0/A_{ef,W3}^m = \exp(-B)^m$ .

For the left-truncated Weibull statistics, the data regression procedure is completely analogous. The expression for the probability of collapse [Eq. (29)] leads to

$$P_{f,WT} = 1 - \exp\left[-\frac{K_{TW}\sigma_{max}^m - \sigma_0^m}{\eta_0^m} A\right]$$

$$\Rightarrow \ln\left[A\frac{\sigma_0^m}{\eta_0^m} + \ln\left(\frac{1}{1 - P_{f,WT}}\right)\right] = m \ln(\sigma_{max}) + \ln\left(\frac{A_{ef,WT}}{\eta_0^m}\right) \quad (49)$$

where now the expression for  $A_{ef,WT}$  is given by Eq. (30). It is worth recalling that, since also the equivalent stress  $\sigma_{eq,WT}$  takes the same form of the 2PW case, the discussion follows the same rationale given for the 2PW statistics. In particular, the variation of  $A_{ef,WT}$  is associated with nonlinear geometric effects only; therefore, at least as a first-order approximation, it can be assumed to be constant for all the measured strengths.

One can then define  $G = A\sigma_0^m/\eta_0^m$ ,  $B = \ln[A_{ef,WT}/\eta_0^m]$ ,  $y = \ln[G + \ln 1/(1 - P_{f,WT})]$  and  $x = \ln \sigma_{max}$ . The expression 2 in

Eq. (49) can be thus written as  $y = mx + B$ . Then, under the hypothesis  $A_{ef,WT} = \text{const}$ , the problem consists in finding the value of  $G$  such that, in the LTW plane  $\ln[G + \ln 1/(1 - P_f)]$  versus  $\ln(\sigma)$ , the resulting points are best aligned. From the linear interpolation of the data, one finds the optimal value of  $m$  and  $B$ . The other parameters can thus be obtained as

$$\eta_0 = A_{ef,WT}^m [\exp(-B)]^{1/m};$$

$$\sigma_0 = \eta_0 \left(\frac{G}{A}\right)^{1/m} = [K_{TW} \exp(-B)G]^{1/m} \quad (50)$$

The corresponding plots in the LTW plane, with the corresponding interpolating lines of the data of (CEN 2006), are shown in Fig. 9 for the air- and tin-side surfaces.

The values of the Weibull parameters for the 2PW, 3PW, and LTW, obtained by the linear regression procedures just outlined, are summarized in Table 1. Notice that the method permits to directly estimate the quantity  $\eta_{0,air}/A_{ef}^m$ , which has the dimensions of force per unit area, but estimation of the value of collocation parameter  $\sigma_0$  for the LTW distribution requires the knowledge of  $K_{TW}$ . For the testing configuration (CEN 2001a), neglecting second-order effects, one can assume (Pisano and Royer-Carfagni 2015a, Fig. 6) that  $K_{TW} = 0.5$  for the air side and  $K_{TW} = 0.45$  for the tin side.

It is observed in Figs. 8 and 9 that there is not a substantial difference in the possibility of fitting the experimental data between the 3PW and LTW statistics. However, the evaluation of the equivalent state of stress for the 3PW statistics, according to either Eq. (18) or Eq. (19), is not without ambiguity. Moreover, also the definition of the effective area  $A_{ef,W3}$  according to Eq. (22) is much more complicated than for the LTW approach. A final remark is that the Weibull shape parameter  $m$  for the 3PW distribution results to be much smaller than for the other two cases.

### Weibull Distributions without a Lower Bound

Consider first the bilinear Weibull (BLW) distribution. The intrinsic difficulties for the definition of the effective area  $A_{ef,WL}$ , associated with the presence of two set of Weibull moduli, have been

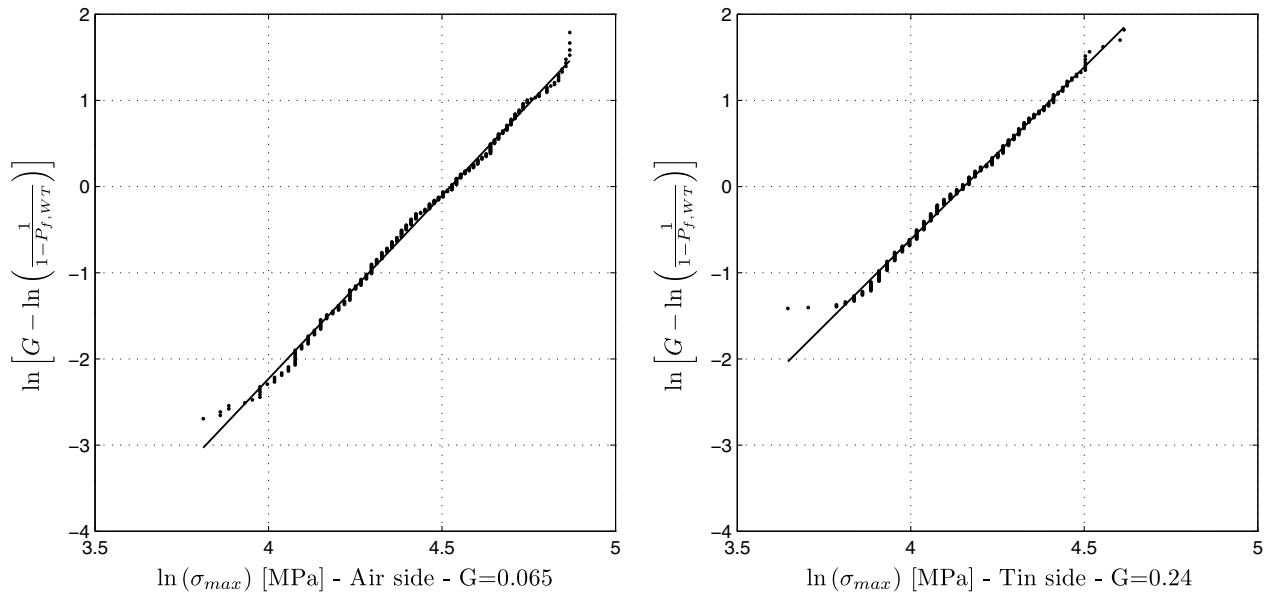


**Fig. 9.** Linear interpolation in the LT Weibull plane  $\ln[G + \ln 1/(1 - P_f)]$  versus  $\ln(\sigma)$  of the failure stress measurements by CEN/TC129/WG8; distinction between tin-side and air-side measurements

discussed already. A model of the type [Eq. (34)] would be very hard to treat, and this is why here it is necessary to limit the assumption that the statistical distribution is given by Eq. (33). The corresponding statistics is consequently of the form

$$P_{f,WL} = \begin{cases} 1 - \exp\left[-\left(\frac{\sigma_{\max}}{\eta_1}\right)^{m_1} A_{ef,WL,1}\right] & \text{for } 0 < \sigma_{\max} \leq \sigma^* \\ 1 - \exp\left[-\left(\frac{\sigma_{\max}}{\eta_2}\right)^{m_2} A_{ef,WL,2}\right] & \text{for } \sigma_{\max} > \sigma^* \end{cases} \quad (51)$$

where  $A_{ef,WL,1}$  and  $A_{ef,WL,2}$  = values of the effective area on the branches  $\sigma_{\max} \leq \sigma^*$  and  $\sigma_{\max} > \sigma^*$  according to the definition of Eq. (36). Neglecting geometric nonlinear effects, one can assume that the aforementioned values are constant for any value of  $\sigma_{\max}$ , apart from the jump that they exhibit when  $\sigma_{\max} = \sigma^*$ . Since one has indeed two distinguished 2PW distributions, the plane useful to perform the linear regression of the data is obviously the same used for the 2PW statistics. The data are split into two series according to the value of  $\sigma^*$  and the four parameters characterizing the BLW statistics have been estimated by the linear regression of the data contained in each of the two resulting domains. The choice of  $\sigma^*$  has been made so to maximize the goodness of fit. For the tin and air sides, they are, respectively,  $\sigma_{\text{tin}}^* = 63.46$  MPa and  $\sigma_{\text{air}}^* = 52.12$  MPa.

The analysis for the bimodal Weibull distribution has been made using the expression Eq. (52) for  $\hat{P}_{f,WM}$ , with the corresponding

definition in Eq. (40) for the effective area  $\hat{A}_{ef,WM} = K_{WM}A$ , so that the resulting expression is of the type

$$\hat{P}_{f,WM} = 1 - \exp\left[-\left(\frac{\sigma_{\max}}{\eta_1}\right)^{m_1} \hat{A}_{ef,WM}\right] - \exp\left[-\left(\frac{\sigma_{\max}}{\eta_2}\right)^{m_2} \hat{A}_{ef,WM}\right] + \exp\left\{-\left[\left(\frac{\sigma_{\max}}{\eta_1}\right)^{m_1} + \left(\frac{\sigma_{\max}}{\eta_2}\right)^{m_2}\right] \hat{A}_{ef,WM}\right\} \quad (52)$$

Note that, in this case, the definition of the effective area is strongly stress dependent. However, in order to evaluate the method, it was decided, as a first attempt, to neglect such a dependence. Then, the best fit is obtained by varying the four parameters of the distribution.

The plots of the best-fit Weibull probability plots obtained by using the BLW and BMW approaches are represented in Fig. 10, making again the distinction between the tin and air side. From a graphical point of view, both the BLW and BMW distributions show a similar capability of fitting the experimental data, so that from the purely statistical point of view, there is not a substantial difference between using one over the other. However, the calculation of the effective area is extremely difficult for both cases, and to the authors' knowledge the two approaches are not corroborated by a sound micromechanically motivated model.

The numerical estimated values of the various parameters characterizing the BLW and the BMW statistics are recorded in Table 2. The method that has been here used to fit the experimental data is essential graphical, but nevertheless it provides useful information. Comparing the data of Table 1 with those of Table 2, observe that the shape parameter  $m$  for the BLW and BMW cases fitting the right-hand-side tail of the data is similar to the value corresponding to the LTW distribution. However, the values of  $m$  predicted on the left-hand-side tail are much higher, of the order of 10 for the air side, and 12/15 for the tin side. There is not a substantial difference between the Weibull parameters obtained with the BLW and BMW distribution, at least for the air side, while the distinction is slightly more evident for the tin side. In conclusion, at least from a

**Table 1.** Weibull Parameters for the 2PW, 3PW, and LTW Statistics, Obtained by Linear Regression of the Experimental Data by CEN/TC129/WG8

Statistics	$m_{\text{air}}$	$m_{\text{tin}}$	$\eta_{0,\text{air}}/A_{ef,\text{air}}^{1/m}$ (MPa)	$\eta_{0,\text{tin}}/A_{ef,\text{tin}}^{1/m}$ (MPa)	$\sigma_{0,\text{air}}$ (MPa)	$\sigma_{0,\text{tin}}$ (MPa)
2PW	5.37	6.45	94.17	68.38	—	—
3PW	2.55	2.65	52.84	31.20	39.00	36.00
LTW	4.00	4.25	58.22	38.04	41.21	36.51

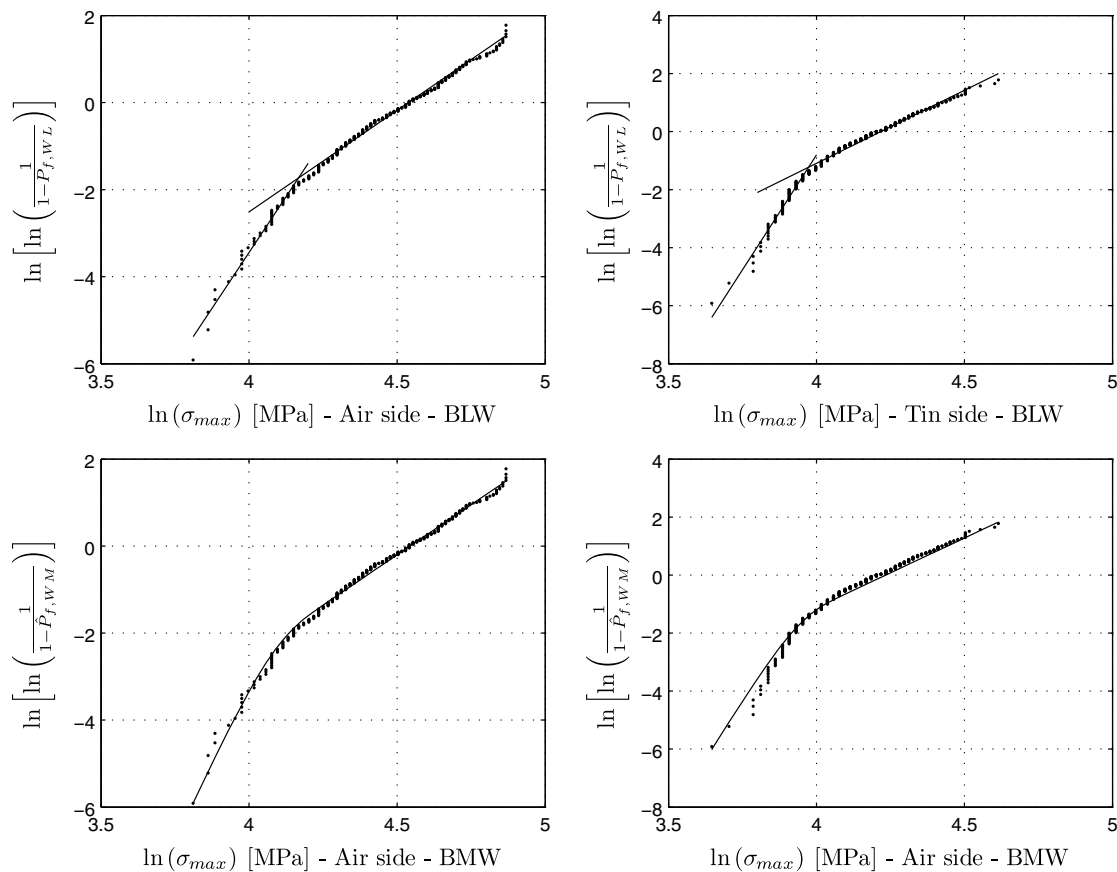


**Fig. 10.** Bilinear and bimodal Weibull probability plots of the failure stress measurements by CEN/TC129/WG8; distinction between tin-side and air-side measurements

**Table 2.** Estimated Weibull Parameters for the BLW and the BMW Statistics, Obtained by Linear Regression of the Experimental Data by CEN/TC129/WG8

Statistics	$m_{\text{air},1}$	$m_{\text{air},2}$	$\eta_{0,\text{air},1}/A_{\text{ef,air}}^{1/m_1}$ (MPa)	$\eta_{0,\text{air},2}/A_{\text{ef,air}}^{1/m_2}$ (MPa)	$m_{\text{tin},1}$	$m_{\text{tin},2}$	$\eta_{0,\text{tin},1}/A_{\text{ef,tin}}^{1/m_1}$ (MPa)	$\eta_{0,\text{tin},2}/A_{\text{ef,tin}}^{1/m_2}$ (MPa)
BLW	10.25	4.62	76.41	94.03	15.83	5.03	57.44	67.84
BMW	10.25	4.62	57.50	94.03	11.80	4.80	50.00	69.00

qualitative point of view, the BLW and the BMW approaches seem to be quite equivalent.

Consider finally the analysis of the extended Weibull (EXW) distribution of Eq. (42). The most important feature of this model is that the effective area  $A_{\text{ef,WE}} = K_{\text{WE}}A$  takes the same expression [Eq. (12)] associated with the 2PW distribution. Therefore, the variations of  $A_{\text{ef,WE}}$  are due to nonlinear geometric effects also for this case, which lead to the same results if they are neglected.

Setting  $y = \ln[\ln(1/(1 - P_f))]$  and  $x = \ln \sigma_{\text{max}}$  and using the equivalence in Eq. (43), it is not difficult to verify (Zhang and Xie 2007) that in the Weibull plane, the probability plot is the smooth curve of equation

$$y = \ln[-(\ln(\nu) - \ln\{\exp[\exp(x)/(\eta_0/A_{\text{ef,WE}}^{1/m})^m - (1 - \nu)]\})] \quad (53)$$

The three parameters of the EXW statistics have been estimated with the same procedure proposed by Zhang and Xie (2007). The corresponding values are  $m_{\text{air}} = 7.9$ ;  $\eta_{0,\text{air}}/A_{\text{ef,WE,air}}^{1/m} = 139$  MPa;  $\nu_{\text{air}} = 0.0151$ ;  $m_{\text{tin}} = 7.9$ ;  $\eta_{0,\text{tin}}/A_{\text{ef,WE,tin}}^{1/m} = 100$  MPa; and

$\nu_{\text{tin}} = 0.012$ . Note that the shape parameter  $m$  is higher than in the 2PW, 3PW, and LTW, but much lower than in the BLW and BMW approaches.

The corresponding graphs have been plotted in Fig. 11. An acceptable goodness-of-fit is observed for the air-side data, whereas the tin-side data are not interpolated well by the statistical model.

### Chi-Square Goodness-of-Fit Test

The chi-square goodness-of-fit test consists in the verification of the null hypothesis  $H_0$ , stating that a particular effect indicated by elaborating a sample is due only to random variation between the sample and the population, i.e., the difference between the expected values from an assigned statistical distribution and the observed data is due to chance alone (Navidi 2008). To perform the test, the data must be grouped into  $k$  classes ( $C_1, C_2, \dots, C_k$ ), which are associated with the observed frequencies ( $n_1, n_2, \dots, n_k$ ). Let  $p_1, p_2, \dots, p_k$  be the probability that a stochastic variable ( $X$ ) assumes a value inside one of the classes according the statistical model under analysis, and ( $np_i, i = 1, 2, \dots, k$ ) be the expected

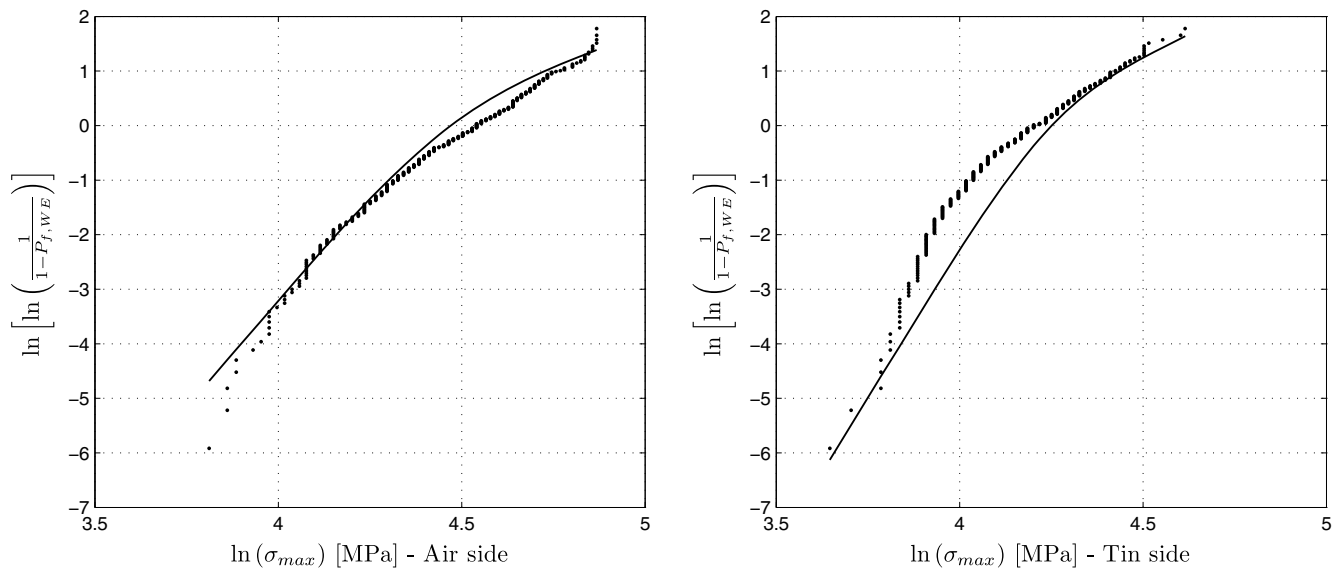


**Fig. 11.** Extended Weibull probability plot of the failure stress measurements by CEN/TC129/WG8; distinction between tin-side and air-side measurements

absolute frequency. A measure of the discrepancy between the observed and the expected frequencies is of the form

$$X_c^2 = \sum_{i=1}^k \frac{(n_i - np_i)^2}{np_i} \quad (54)$$

obviously, the larger the value of  $X_c^2$ , the stronger the evidence against  $H_0$ .

The idea behind the hypothesis test is that if  $H_0$  is true, then the observed and expected values are likely to be close to each other. Therefore, a test statistic can be constructed that measures the closeness of the observed to the expected values. The statistic is called the chi-square statistic and the  $p$ -value is a measure of the probability that the hypothesis  $H_0$  is true. To determine the  $p$ -value for the test, one must know the null distribution of the test statistic [Eq. (54)], i.e., the distribution of the  $X_c^2$  under the hypothesis that  $H_0$  is true. In general, one cannot determine the null distribution exactly, but when the expected values are all sufficiently large, a good approximation is available. It is called the chi-square distribution, denoted by  $\chi_g^2$ , where  $g$  is a number that represents the degree of freedom. If  $n_{\text{par}}$  denotes the number of parameters characterizing the statistical distribution under analysis, then  $g = k - 1 - n_{\text{par}}$ .

This test is sensitive to the chosen number of bins  $k$  in which the data are grouped and to their distribution, but there is not a recognized absolute optimal choice for bin width. Here, it was chosen to group the data into 20 bins of equal width. Since the expected frequencies for each bin should be at least five so to guarantee a good chi-square approximation, here some bins were joined in the tails for some of the analyzed distributions. Once  $X_c^2$  is evaluated and the number of degrees of freedom  $k$  is fixed, the corresponding  $p$ -value can be obtained from the  $\chi_g^2$  distribution using a simple computer algorithm.

An estimate of the goodness-of-fit of the various statistical models can be obtained with this method, which is by far more objective than the simple graphical comparison in the Weibull plane. The  $p$ -values associated with all the distributions under consideration are recorded in Table 3. It is useful to recall that it is

customary to accept the 5% rule, i.e., the  $H_0$  hypothesis is accepted (rejected) if  $p \geq 5\%$  ( $p < 5\%$ ).

The results of Table 3 seem to reinforce the idea of the existence of a lower bound for the float glass strength, since the statistical distributions that provide the location parameter  $\sigma_0$  (3PW, LTW) exhibit an extremely high goodness-of-fit, at least for the air-side data ( $p_{\text{air},3PW} = 0.7332$  and  $p_{\text{air},LTW} = 0.6676$ ). Moreover, it is confirmed that the 2PW is absolutely not sufficient to represent the statistical population of the float glass strength.

If the idea of a lower bound for glass strength is too hard to accept, the BLW and BMW statistics, whose  $p$ -values are still very good ( $p_{\text{air},BLW} = 0.2128$  and  $p_{\text{air},BMW} = 0.2401$ ), could represent a valid alternative. However, for such distributions, the definition of the effective area for specimens with different size and loading conditions presents significant complications. Moreover, the physical justification of such models has not yet been proposed.

The EXW model, which is generally used instead of the 3PW approach because it does not imply a lower bound for glass strength (Hirose 2002), provides a less accurate interpretation of the experimental data for the air side ( $p_{\text{air},EXW} = 0.0979$ ). However the approximation is acceptable according to the 5% rule.

On the other hand, none of the generalized distributions under consideration is able to definitely represent the statistical population of the tin-side strength. The reason for this can be found in the discussion at the end of the section about the existence of a threshold for glass strength, according to which the tin side should be considered a predamaged glass, whose statistic is inevitable affected by a different in type defect population introduced during

**Table 3.** Estimated  $p$ -Values for the Generalized Weibull Distributions under Consideration

Statistics	$p$ -value air	$k$ air	$p$ -value tin	$k$ tin
2PW	$\cong 0$	19	$\cong 0$	16
3PW	0.7332	20	0.0027	16
LTW	0.6676	19	0.003	15
BLW	0.2128	19	0.0235	16
BMW	0.2401	19	0.0041	17
EXW	0.0979	20	$\cong 0$	15

the production process. However, the statistical evaluation of this deviation goes beyond the scope of the present work.

## Discussion and Conclusions

The aim of this article has been to provide a better understanding of the statistical distributions that can be used to model the population of the measured strength of float glass. The attention has been focused on the left-hand-side tails of the cumulative distributions, associated with low strengths and low probabilities of failure because these are the most interesting for high reliability structural applications (Badalassi et al. 2014). The major question that has been addressed here is the following: does a lower bound for the strength of float glass exist? Although a positive response to this statement may go against the common engineering sense, according to which no material can be 100% safe, there are arguments in favor of this conclusion.

The argument for a lower bound strength is buttressed by the statistical analysis of the results from the wide experimental campaign by CEN/TC129/WG8 (CEN 2006), which show that if the data associated with the cumulative probability of failure are plotted in the Weibull plane  $\ln[-\ln(1 - P_f)]$  versus  $\ln(\sigma)$ , the points clearly deviate from linearity in the left-hand-side tail. This is why a two-parameter Weibull distribution, which is by far the most used statistic for brittle material, fails to interpret the experimental evidence for float glass. The strength is much higher than expected from the statistical model whenever the lower branch is attained.

Moreover, there is wealth of experimental evidence that natural aging and the consequent degradation cannot produce a decay of glass strength below a certain limit. This is confirmed by the strength data after sandblasting (Madjoubi et al. 1999), which can be considered to reproduce an extreme condition of aging. A qualitative justification of this finding has been proposed, with arguments based upon micromechanical modeling within the framework of linear elastic fracture mechanics (LEFM). Indeed, the larger preexisting flaws, which characterize the weakest glass specimens, appear to have a bigger size than that of the flaws successively induced by damage. Therefore, these may have a shielding action on the preexisting cracks, as well as an amplification effect, which remains in any case limited.

This study has tried to interpolate the experimental results of glass strength by using generalized statistics like Weibull, presenting a third collocation parameter associated with an assumed lower bound of glass strength. Their ability to interpolate the experimental data has been evaluated by using the chi-square goodness-of-fit test (Navidi 2008), whose associated  $p$ -value represents the probability that the measured discrepancy between observed and expected frequencies is due to chance alone. The three-parameter Weibull distribution and the left-truncated Weibull distributions both provide excellent results, especially for the air side of the glass surface.

However, since the hypothesis of a lower bound for glass strength is hard to accept, an attempt has been made to fit the experimental results with unbounded distributions. In particular, the bilinear and bimodal Weibull distributions permit to split the data into various branches and to treat them separately. The  $p$ -values associated with these distributions remain acceptable for the air side, but are much smaller than for the bounded distributions. On the other hand, the bilinear and bimodal functions are very difficult to treat, essentially because they prescribe two distinct values of the shape parameter  $m$ . They present a very complicated rescaling to take into account effects of size and state of stress, and they are not defined on the basis of an underlying micromechanically

motivated model. Although their use has been proposed by some authors, as it is they just seem an easy way to interpolate any graph whose tails present two distinct asymptotic trends.

A further attempt has been made to use a form of extended Weibull statistics, which has been proposed (Marshall and Olkin 1997) to interpret a bimodal behavior. The major advantage of this, with respect to the others, is that it has only one shape parameter  $m$ . This simplifies the calculations, but implies as well that the tails of the distribution in the Weibull plane tend to present the same slope, a finding that can be weakly appreciated in the glass data. The corresponding  $p$ -value confirms that the result are not satisfactory, not even for the air-side surface.

It is the authors' opinion that the statistical treatment of the experimental evidence is in favor of the conjecture that there is a lower bound for glass strength. This possibility has been attributed to the presence of strict controls in the float glass production process. These must guarantee the quality of the material and, implicitly, assure on a statistical basis that there are no flaws above a certain dimension. Elementary considerations of LEFM confirm that the lower bound of glass strength deduced from experiments is compatible with the maximum size of flaws that have been detected, in agreement with the prescriptions of product standards for float glass.

Since the assumed limit value for glass strength is associated with the opening of the largest cracks that can be found in glass, such a value should be rescaled to take into account modification of their shape and size. In particular, the well-known phenomenon of subcritical crack propagation (static fatigue) implies that the limit strength depends upon the loading time. Moreover, this paper also discussed how natural abrasion/erosion can increase the stress intensity factor of existing flaws under particular conditions, but never above a certain threshold, if not producing a shielding effect.

None of the considered generalized Weibull statistics provides a remarkable goodness-of-fit for the tin side of the glass. This can be attributed to the fact that the tin side represents an example of a damaged surface, whose degradation with respect to the air side (the pristine surface) is due to the contact with the tin bath, and even more so with the supporting rollers during the float production process. In order to achieve a better representation of the tin-side strengths, a more elaborated statistics taking into account the effects of damage should be used. In fact, it is plausible that the artificially induced damage does not follow a Weibull-like approach, but this analysis will be the subject of future work.

In any case, the present study suggests that the left-truncated Weibull distribution appears to be the one that is able, much better than the others, to interpolate the experimental results. This statistical model has its direct justification in the factory production controls, which reject those glass with defects above a certain limit. Moreover, the rescaling due to size and stress effects is much easier than for the three-parameter Weibull distribution. In addition, the three-parameter Weibull distribution would indeed contradict a wealth of literature (Bažant and Pang 2007; Le and Bažant 2011; Salviato and Bažant 2014), which showed that, without left truncation, the probability of the left tail should follow a power law.

Obviously, all the aforementioned considerations depend upon statistics, whose results are in general accurate when simple descriptors, like the mean value or the standard deviation, are considered. The treatment of the extreme values and the characterization of the tails of the distributions, which indeed are of importance in structural calculations, is less obvious. Accepting a lower bound for glass strength represents a major step change, which certainly requires further verifications, especially at the experimental level, before being incorporated in structural standards. Do not forget that

the statistician who confidently tried to cross a river that was 1 m deep, on average, inevitably drowned.

## Appendix. Micromechanically Motivated Model of Glass Strength

It is widely accepted (Ciccotti 2009) that the brittle response of float glass is due to surface microcracks, which unboundedly propagate in Mode I once the positive crack opening stress reaches the critical value. Therefore, most models in LEFM consider the response of an equivalent dominant crack, whose plane is at right angle to the glass surface and randomly oriented. Crack growth is governed by the SIF in Mode I

$$K_I = \sigma_g Y \sqrt{\pi c} \quad (55)$$

where  $c$  = minor axis of the crack, supposed to be semielliptical;  $\sigma_g$  = tensile macroscopic normal component of stress, orthogonal to the crack plane; and  $Y$  = shape factor, which takes into account the aspect ratio of the ellipse. Instantaneous collapse occurs when the SIF reaches the critical threshold  $K_{Ic}$ , which for float glass is of the order of  $K_{Ic} = 0.75 \text{ MPa m}^{0.5}$  (Wiederhorn 1969).

However, glass experiences a very subtle phenomenon usually referred to as static fatigue or subcritical crack growth (Wiederhorn and Bolz 1970), according to which surface microflaws can slowly grow over time even when their size is far below the critical size. In the intermediate asymptotic regime of propagation, the crack shape tends to become semicircular, so that in Eq. (55) it is usually assumed that  $c$  is the radius of the crack and  $Y = 2.24/\pi$ . The speed of subcritical crack growth is traditionally considered a function of the SIF, governed by a power law (Evans 1978) of the type

$$\frac{dc}{dt} = \nu_0 \left( \frac{K_I}{K_{Ic}} \right)^n \quad (56)$$

where  $\nu_0$  and  $n$  depend upon the thermo-hygrometric conditions and the type of glass (Wiederhorn et al. 1982). For float glass, it is customary to assume  $\nu_0 = 0.0025 \text{ m/s}$  and  $n = 16$ , to remain on the safe side. More precisely, subcritical propagation occurs when the SIF is above a lower bound  $K_{I0}$ , but since this is usually quite low, one can safely assume  $K_{I0} = 0$  and consider Eq. (56) to be valid when  $0 \leq K_I \leq K_{Ic}$ .

Denoting with  $\sigma_{\perp}$  the component of stress normal to the crack plane, when failure occurs at  $\sigma_{\perp} = f_c$ , the corresponding critical crack size is  $c_c = [K_{Ic}/Yf_c\sqrt{\pi}]^2$ . In a generic load history  $\sigma_{\perp} = \sigma(t)$ , using Eqs. (55) and (56), one can write

$$\int_{c_i}^{c_c} c^{-n/2} dc = \int_0^{t_f} \nu_0 \left( \frac{\sigma(t) Y \sqrt{\pi}}{K_{Ic}} \right)^n dt \quad (57)$$

where  $t_f$  represents the failure time, when the measured value of  $f_c$  is  $f_{\text{test}}$  and, correspondingly,  $c = c_c$ , whereas  $c_i$  is the initial size of the dominant crack, which represents an effective measure of the initial defectiveness. Since tests are as a rule performed at constant stress rate  $\dot{\sigma}$ , then  $\sigma(t) = \dot{\sigma} t$  and  $t_f = f_{\text{test}}/\dot{\sigma}$ . Then, Eq. (57) can be easily integrated to give

$$c_i = \left[ \frac{n-2}{2} \frac{\nu_0}{n+1} \left( \frac{Y\sqrt{\pi}}{K_{Ic}} \right)^n \frac{f_{\text{test}}^{n+1}}{\dot{\sigma}} + \left( \frac{Y f_{\text{test}} \sqrt{\pi}}{K_{Ic}} \right)^{n-2} \right]^{2/(n-2)} \quad (58)$$

Consideration of the order of magnitudes of the various quantities indicates that the second term in this expression is much smaller than the first one. Observe, in passing, that within this

approximation, if all specimens had the same initial defect  $c_i$ , then  $f_{\text{test}}^{n+1}/\dot{\sigma} = R$  would be a constant, whatever the stress rate  $\dot{\sigma}$  used in the test. This observation is at the basis of the experimental method proposed by ASTM C1368 (ASTM 2001) to experimentally measure the value of  $n$ , consisting in performing tests at different stress rates.

For design purposes, actions are modeled by constant loads acting on the elements for an effective time, representative of their cumulative effect during their lifetime. If failure occurs after the time  $\tau$  under the constant stress  $\sigma_{\perp} = \sigma_{\tau}$ , by integrating Eq. (57) with  $\sigma(t) = \sigma_{\tau}$  and  $t_f = \tau$ , one obtains (Badalassi et al. 2014)

$$\sigma_{\tau}^n \tau = \frac{2/(n-2)c_i^{(2-n)/2}}{\nu_0 \left( \frac{Y\sqrt{\pi}}{K_{Ic}} \right)^n} = \frac{1}{n+1} R \quad (59)$$

A practical way to take into account of this phenomenon is to formally reduce the reference strength of glass according to the coefficient  $k_{\text{mod}}$ . More specifically, if  $f_{\text{ref}}$  is the reference strength for glass, traditionally measured from tests at constant stress rate  $\dot{\sigma}_{\text{ref}} = 2 \text{ MPa/s}$ , then the reference strength  $\sigma_{\tau}$  for a stress constantly applied for the time  $\tau$  is  $\sigma_{\tau} = k_{\text{mod}} f_{\text{ref}}$ , where from Eq. (59)  $k_{\text{mod}}$  reads

$$k_{\text{mod}} = \frac{\sigma_{\tau}}{f_{\text{ref}}} = \frac{1}{f_{\text{ref}}} \left( \frac{1}{n+1} \right)^{1/n} \left( \frac{\tau}{R} \right)^{-1/n} \\ = \left( \frac{1}{n+1} \right)^{1/n} (R)^{1/[n(n+1)]} (\dot{\sigma}_{\text{ref}})^{-1/(n+1)} (\tau)^{-1/n} \quad (60)$$

Using characteristic values for float glass, and in particular  $n = 16$ , one obtains  $k_{\text{mod}} = 0.585(\tau)^{-1/16}$ , where  $t$  is measured in seconds.

## Acknowledgments

The authors acknowledge the support of the Italian Dipartimento della Protezione Civile under project ReLUIS-DPC 2014-2018.

## References

- ASTM. (2001). "Standard test method for determination of slow crack growth parameters of advanced ceramics by constant stress-rate flexural testing at ambient temperature." *ASTM C1368-01*, West Conshohocken, PA.
- ASTM. (2009). "Standard test method for monotonic equibiaxial flexural strength of advanced ceramics at ambient temperature." *ASTM C1499-09*, West Conshohocken, PA.
- Badalassi, M., Biolzi, L., Royer-Carfagni, G., and Salvatore, W. (2014). "Safety factors for the structural design of glass." *Constr. Build. Mater.*, *55*, 114–127.
- Basu, B., Tiwari, D., Kundu, D., and Prasad, R. (2009). "Is Weibull distribution the most appropriate statistical strength distribution for brittle materials?" *Ceram. Int.*, *35*(1), 237–246.
- Batdorf, S., and Heinisch, H., Jr. (1978). "Weakest link theory reformulated for arbitrary fracture criterion." *J. Am. Ceram. Soc.*, *61*(7–8), 355–358.
- Bažant, Z. P., and Pang, S. (2007). "Activation energy based extreme value statistics and size effect in brittle and quasibrittle fracture." *J. Mech. Phys. Solids*, *55*(1), 91–131.
- CEN (European Committee for Standardization). (2001a). "Glass in building—Determination of bending strength of glass. Part 2: Coaxial double ring test on flat specimens with large test surface areas." *EN1288-2. CEN/TC129*, Brussels, Belgium.

- CEN (European Committee for Standardization). (2001b). "Glass in building—Determination of the bending strength of glass." *EN1288. CEN/TC129*, Brussels, Belgium.
- CEN (European Committee for Standardization). (2001c). "Glass in building—Determination of the bending strength of glass. Part 5: Coaxial double ring test on flat specimens with small test surface areas." *EN1288-5. CEN/TC129*, Brussels, Belgium.
- CEN (European Committee for Standardization). (2005). "Basis of structural design." *Eurocode 0—EN1990. CEN-TC250*, Brussels, Belgium.
- CEN (European Committee for Standardization). (2006). "An overview of prEN-13474 and the work of CEN/TC129/WG8 from which it was developed." *CEN/TC129/WG8*, Brussels, Belgium.
- Choi, S., Powers, L., and Nemeth, N. (2000). "Slow crack growth behavior and life/reliability analysis of 96wt alumina at ambient temperature with various specimen/loading configurations." *NASA Technical Memorandum 210206*, Glenn Research Center, Cleveland.
- Ciccotti, M. (2009). "Stress-corrosion mechanisms in silicate glasses." *J. Phys. D. Appl. Phys.*, 42(21), 214006–2140068.
- Cohen, A. C. (1965). "Maximum likelihood estimation in the Weibull distribution based on complete and on censored samples." *Technometrics*, 7(4), 579–588.
- Coleman, B. (1958). "On the strength of classical fibres and fibre bundles." *J. Mech. Phys. Solids*, 7(1), 60–70.
- Collini, L., and Royer-Carfagni, G. (2014). "Flexural strength of glass-ceramic for structural applications." *J. Eur. Ceram. Soc.*, 34(11), 2675–2685.
- Danzer, R. (2006). "Some notes on the correlation between fracture and defect statistics: Are Weibull statistics valid for very small specimens?" *J. Eur. Ceram. Soc.*, 26(15), 3043–3049.
- Durchholz, M., Goer, B., and Helmich, G. (1995). "Method of reproducibly predamaging float glass as a basis to determine the bending strength." *Glastech. Ber. Glass Sci. Technol.*, 68(8), 251–252.
- Evans, A. G. (1978). "A general approach for the statistical analysis of multiaxial fracture." *J. Am. Ceram. Soc.*, 61(7–8), 302–308.
- FRANC3D version 2.6 [Computer software]. Cornell Fracture Group, Ithaca, NY.
- Franco, A., and Royer-Carfagni, G. (2015). "Critical issues in the design-by-testing of glass structures." *Eng. Struct.*, 99, 108–119.
- Freudenthal, A. (1968). *Fracture, an advanced treatise*, Vol. 2, Academic Press, New York, 591–619.
- Hirose, H. (2002). "Maximum likelihood parameter estimation in the extended Weibull distribution and its applications to breakdown voltage estimation." *IEEE Trans. Dielectr. Electr. Insul.*, 9(4), 524–536.
- Klein, C. (2011). "Flexural strength of infrared-transmitting window materials: Bimodal Weibull statistical analysis." *Opt. Eng.*, 50(2), 023402.
- Le, J., and Bažant, Z. P. (2011). "Unified nano-mechanics based probabilistic theory of quasibrittle and brittle structures: II. Fatigue crack growth, lifetime and scaling." *J. Mech. Phys. Solids*, 59(7), 1322–1337.
- Le, J. L., Ballarini, R., and Zhu, Z. (2015). "Modeling of probabilistic failure of polycrystalline silicon mems structures." *J. Am. Ceram. Soc.*, 98(6), 1685–1697.
- Lindqvist, M., and Lebet, J. P. (2014). "Strength of glass determined by the relation of the critical flaw to the fracture mirror." *Eng. Fract. Mech.*, 119, 43–52.
- Madjoubi, M., Bousbaa, C., Hamidouche, M., and Bouaouadja, N. (1999). "Weibull statistical analysis of the mechanical strength of a glass eroded by sand blasting." *J. Eur. Ceram. Soc.*, 19(16), 2957–2962.
- Marshall, A., and Olkin, I. (1997). "A new method for adding a parameter to a family of distributions with application to the exponential and Weibull families." *Biometrika*, 84(3), 641–652.
- Munz, D., and Fett, T. (1999). *Ceramics: Mechanical properties, failure behaviour, materials selection*, Springer, Berlin.
- Navidi, W. (2008). *Statistics for engineers and scientists*, McGraw-Hill, New York.
- Nurhuda, I., Lam, N., Gad, E., and Calderone, I. (2010). "Estimation of strengths in large annealed glass panels." *Int. J. Solids Struct.*, 47(18–19), 2591–2599.
- Overend, M., and Louter, C. (2015). "The effectiveness of resin-based repairs on the inert strength recovery of glass." *Constr. Build. Mater.*, 85, 165–174.
- Phani, K., and De, A. (1987). "A flaw distribution function for failure analysis of brittle materials." *J. Appl. Phys.*, 62(11), 4433–4437.
- Pisano, G., and Royer-Carfagni, G. (2015a). "The statistical interpretation of the strength of float glass for structural applications." *Constr. Build. Mater.*, 98, 741–756.
- Pisano, G., and Royer-Carfagni, G. (2015b). "Towards a new standardized configuration for the coaxial double test for float glass." *Eng. Struct.*, 119, 149–163.
- Pourreux, C. (1997). "Strength of glass eroded by round particles." *Technical Rep. No. 29–97*, Philips Electronics, Amsterdam, Netherlands.
- Przybilla, C., Fernández-Canteli, A., and Castillo, E. (2011a). "An iterative method to obtain the specimen-independent three-parameter Weibull distribution of strength from bending tests." *Procedia Eng.*, 10, 1414–1419.
- Przybilla, C., Fernández-Canteli, A., and Castillo, E. (2011b). "Deriving the primary cumulative distribution function of fracture stress for brittle materials from 3- and 4-point bending tests." *J. Eur. Ceram. Soc.*, 31(4), 451–460.
- Rickerby, D. (1980). "Theoretical aspects of the statistical variation of strength." *J. Mater. Sci.*, 15(10), 2466–2470.
- Rodichev, Y., Yevplov, Y., Soroka, H., Veer, F., Tregubov, N., and Polivyany, V. (2012). "Surface defects and statistical characteristics of glass strength." *Challenging Glass 3—Conf. on Architectural Structure Applications Glass*, F. Bos, C. Louter, R. Nijse, and F. Veer, eds., IOS Press, Amsterdam, Netherlands, 535–552.
- Salviato, M., and Bažant, Z. P. (2014). "The asymptotic stochastic strength of bundles of elements exhibiting general stress-strain laws." *Probabilist. Eng. Mech.*, 36, 1–7.
- Salviato, M., Kirane, K., and Bažant, Z. (2014). "Statistical distribution and size effect of residual strength of quasibrittle materials after a period of constant load." *J. Mech. Phys. Solids*, 64, 440–454.
- Vandebroek, M., Louter, C., Caspeele, R., Ensslen, F., and Belis, J. (2014). "Size effect model for the edge strength of glass with cut and ground edge finishing." *Eng. Struct.*, 79, 96–105.
- Wang, Z., Liu, L., Li, X., and Zhao, L. (2010). "An experimental method for analyzing environmental effects of blowing sands on glass abrasion." *Procedia Environ. Sci.*, 2, 207–217.
- Weibull, W. (1939). "A statistical theory of the strength of materials." *Ingeniörsvetenskapsakademiens Handlingar*, 151, 1–45.
- Weibull, W. (1951). "A statistical distribution function of wide applicability." *J. Appl. Mech.*, 18, 293–297.
- Wereszczak, A., Ferber, M., and Musselwhite, W. (2014). "Method for identifying and mapping flaw size distributions on glass surfaces for predicting mechanical response." *Int. J. Appl. Glass Sci.*, 5(1), 16–21.
- Wiederhorn, S. (1969). "Fracture surface energy of glass." *J. Am. Ceram. Soc.*, 52(2), 99–105.
- Wiederhorn, S., and Bolz, L. (1970). "Stress corrosion and static fatigue of glass." *J. Am. Ceram. Soc.*, 53(10), 543–548.
- Wiederhorn, S. M., Freiman, S. W., Fuller, E., Jr., and Simmons, C. (1982). "Effects of water and other dielectrics on crack growth." *J. Mater. Sci.*, 17(12), 3460–3478.
- Xiao, X., and Yan, X. (2008). "A numerical analysis for cracks emanating from a surface semi-spherical cavity in an infinite elastic body by FRANC3d." *Eng. Fail. Anal.*, 15(1–2), 188–192.
- Yankelevsky, D. (2014). "Strength prediction of annealed glass plates—A new model." *Eng. Struct.*, 79, 244–255.
- Zhang, T., and Xie, M. (2007). "Failure data analysis with extended Weibull distribution." *Commun. Stat. B-Simul.*, 36(3), 579–592.